On the effect of spatial sampling in damage detection of cracked beams by continuous wavelet transform

Elsevier Editorial System(tm) for Journal of Sound and Vibration
Manuscript Draft

Manuscript Number: JSV-D-14-00633R1

Title: ON THE EFFECT OF SPATIAL SAMPLING IN DAMAGE DETECTION OF CRACKED BEAMS BY CONTINUOUS WAVELET TRANSFORM

Article Type: Full Length Article

Section/Category: K Signal processing for sound and vibration applications

Keywords: spatial sampling interval; down-sampling; vibration-based damage identification; wavelet analysis; CWT; padding method; cracked beam

Corresponding Author: Prof. A. Spagnoli, Ph.D.

Corresponding Author's Institution: University of Parma

First Author: Lorenzo Montanari, PhD

Order of Authors: Lorenzo Montanari, PhD; A. Spagnoli, Ph.D.; Biswajit Basu, Prof.; Brian Broderick, Prof.

Abstract: Modern measurement techniques are improving in capability to capture spatial displacement fields occurring in deformed structures with high precision and in a quasi-continuous manner. This in turn has made the use of vibration-based damage identification methods more effective and reliable for real applications. However, practical measurement and data processing issues still present barriers to the application of these methods in identifying several types of structural damage. This paper deals with spatial Continuous Wavelet Transform (CWT) damage identification methods in beam structures with the aim of addressing the following key questions: (i) can the cost of damage detection be reduced by down-sampling? (ii) what is the minimum number of sampling intervals required for optimal damage detection ? The first three free vibration modes of a cantilever and a simple supported beam with an edge open crack are numerically simulated. A thorough parametric study is carried out by taking into account the key parameters governing the problem, including the wavelet mother function, level of noise, crack depth and location, mechanical and geometrical parameters of the beam and the use of a padding method to reduce border distortions. The results are employed to assess the optimal number of sampling intervals for effective damage detection.

18 November 2014

Ms. Ref. No.: JSV-D-14-00633

Title: ON THE EFFECT OF SPATIAL SAMPLING IN DAMAGE DETECTION OF CRACKED BEAMS BY CONTINUOUS WAVELET TRANSFORM

Journal of Sound and Vibration

Reviewer #2: The paper presents a parametric study to analyse the effect of spatial sampling in damage detection of cracked beams by continuous wavelet transform (CWT).
The paper is interesting and illustrates clearly a topic of relevance in the field of Structural Health Monitoring. However, before publishing can be recommended, a number of clarifications, improvements and corrections would be appropriate regarding the following points:

1) The normalised sampling intervals considered are equal to 0.025, 0.01, 0.005, 0.0025, 0.001,
0.0005 and 0.00025. This means that for the beam used in the example, which is one meter long, the distance between two sensors is 25 mm (40 measurement points considered along the beam) 10mm (100 points), 2.5mm (400 points), 1mm (1000 points), 0.5mm (2000 points), 0.25mm (4000 measurement points). In this reviewer opinion, it is not realistic to consider the last three intervals because even with latest measurement techniques, such as a scanning laser vibrometer, it is very difficult to achieve the required level of precision due to the limits of the instrumentation, test setup, operator, etc. Instead it should be more interesting and appropriate to consider larger sampling intervals (eg 0.04 and 0.05) in order to understand whether or not the CWT can still be applied for the damage localisation purpose.

We agree with the Reviewer that, for a 1m-long beam, normalized sampling intervals of 0.001, 0.0005 and 0.00025 would yield unrealistic distances between measurement points. However, the trend of results being presented is preserved even if one does not consider such smallest intervals. The values of sampling intervals was selected in order to explore a sampling interval range as large as possible (sampling intervals equal to 0.04 and 0.05 were excluded from the analysis because they correspond, when the crack is located at 0.1L or 0.9L, to an insufficient number, for wavelet transform, of sampling points laying between the crack and the nearby beam end).
A sentence has been added to warn the reader that the selected smallest sampling intervals might lead to unrealistic measurement spacing.

2) In the text the following parameters are used ß1, ß2, H1, H1(overlined) H2, H2(overlined) referring to a different paper. As the article should be self-contained without being too repetitive, the meaning of these parameters should be shortly explained.

The sentence has slightly been modified to explain these parameters:
'By using the polynomial padding method [31], the damage identification turns out to be, with good approximation, a function of the pseudo-frequency only (in the simulations of Fig. 6 the fitting parameters of the method are assumed to be $\beta_1 = \beta_2 = 1$, $H_1 = \overline{H}_1$ and $H_2 = \overline{H}_2$).'

3) In the first lines of page 22, it is stated that "As for the beam parameter h, it can be demonstrated [31] that its variation influences the

detectable crack depth but not the optimal pseudo-frequency value of CWT damage detection". However looking at paper [31], this demonstration is not found.

There was a mistake in the number of the reference. The correct reference is [35].

4) As regards the example in section 5, concerning the monitoring of the service state of a wind turbine blade of length 50 m with the CWT, there are two objections. The first one regards the infeasibility of measuring the mode shapes or operational deflection shapes of a real wind turbine blade in-service using laser devices (otherwise which devises the authors would suggest to use?). Moreover, even when out-of-service, since the blade is huge, it is not very realistic to use, a scanning laser vibrometer that would need to be positioned at a distance adequate to the size of the object examined and so very far from the blade. The second one regards the fact that, due to the dimensions, it is rather simplistic to consider only one row of sensors in the longitudinal direction to determine the deflection shapes.

Possibly, the example of a wind turbine blade might not be as appropriate due to the practical measurement implications stated by the Reviewer (incidentally, the bending of a blade is unsymmetrical and two displacement components would be needed to describe its deflection). The purpose of the example is to offer some numerical values of the optimum sampling interval for a given beam size. In the revised version of the manuscript, to avoid any reference to a specific structure, an example of a generic 5m-long cantilever beam is presented.

5) Since there are a lot of diagrams and the reader can get confused, it would be very useful to summarise the fundamental results in a table for each damage case analysed in which the value of the minimum detectable crack size is reported as function of the normalised sampling interval, the noise level, the wavelet function, the kind of mode shape of the beam etc.

The aim of the paper is to investigate the effect of sampling interval on spatial CWT damage detection and to find the optimal sampling interval to identify the minimum detectable crack size. A summary of the results illustrated by Figs 3-9 is reported in Section 4.6 'Discussion of the results', that is

'Focusing on the results of Sections 4.2 – 4.5, pertaining to the use of the polynomial padding method and the 'Coif4' wavelet, the following conclusions can be drawn:

(i) there is an optimal value of pseudo-frequency, independent of the noise level, which maximizes the performance of the damage detection for a given beam deflection shape and crack position;
(ii) by adjusting the wavelet scale, damage detection performances can be similar for small and large sampling intervals.'

The authors believe that the summary table suggested by the Reviewer, in which the values of minimum detectable crack size would be reported as a function of some problem parameters (SNR, wavelet function, mode shape, etc.), would be misleading with respect to the main goal of the paper.

In addition, the values of minimum detectable crack size appearing in Figs 3-9 are related to the specific beam considered in the parametric study ('In this Section, a cracked beam of length L = 1 m with a rectangular cross-section of height h = 0.05L and width b =

0.5*h*, constituted by an elastic linear isotropic material of Young modulus *E* = 200 GPa and density ρ = 7850 kg/m^3, is considered'), and, conversely to the results pertaining to the optimal sampling intervals, they cannot be generalized.

6) According to the curves of Fig. 12, for a given wavelet scale, the optimal number of sampling intervals needed to detect the smallest crack located at different positions along the beam using a given beam vibration mode shape is plotted. However, the value of the smallest crack is not reported and presumably varies depending on the location of the crack. It would be helpful, therefore, to understand the interval range in which this minimum size detectable falls for each plot.

As explained in Section 5 'Generalization of the results', the optimal pseudo-frequency $f_{a,opt}$ multiplied by the beam length L is only a function of the beam deflection shape and of the relative crack position x_c/L. On the contrary, the minimum detectable crack size is a (non-linear) function of the geometric (b,h,L) and mechanical (E) parameters of the beam. Therefore, it is not possible to give an interval range in which the minimum detectable crack size (expressed in terms of relative crack depth δ) would fall for each curve of Fig. 12.
A generalization of results of minimum detectable crack size might be pursued if one express damage extension as a function of a parameter expressing the relative rotational stiffness of the cracked beam section (e.g. $(EI/L)/k_c$), but this is beyond the scope of the present paper.

7) It is suggested to write "mode shapes" instead of the word "modeshapes"

Done.

8) Before equation 4 (which should be 3.7, following the numeration criterion given by the authors), in the sentence "the local stiffness kc due to the crack is evaluated … through the following polynomial expression", the word "polynomial" should be deleted as the polynomial appears in the denominator in formula 4. Furthermore equation 4 should be corrected as in the numerator tb^2 should be bh^2.

Done.

9) For the sampling step, it would be better to use the symbol <DELTA>x instead of dx which is a differential.

Done.

Reviewer #3: The authors present the spatial Continuous Wavelet Transform (CWT) damage identification method in beam structures to evaluate the optimal number of sampling intervals for effective damage detection. The authors investigate some effects due to the wavelet mother function, level of data noise, crack depth and location, mechanical and geometrical beam parameters and the use of a padding method to reduce border distortions. The only concern is some misprints, for example

1)In line 5 on page 6 "modeshapes", should there have a space between two words, such as "mode shapes" or "modal shapes"? Please check the misprints carefully throughout the manuscript for it.

Done.

2)In the last paragraph on page 11, "0.6957 for 'Coif4', 0.6667 for 'Db2', 0.318 for 'Gaus4' and 0.8125 for 'Morl')."? It is better to give the readers a reference or at least introduce briefly how to obtain these values. Please indicate clearly in the text.

As stated in the text, the center frequency is defined as the the frequency maximizing the Fourier transform of the mother wavelet modulus. A reference has been added in the revised version of the manuscript.

3)On page 20 "Since the material density <rho> affects the natural frequencies of the cracked beam but not its mode shapes, this beam parameter turn out to be negligible." It is unclear for this statement, could you give a more clear explanation.

The relevant text has been modified to better explain this point.

Revised version, 18 November 2014

ON THE EFFECT OF SPATIAL SAMPLING IN DAMAGE DETECTION OF CRACKED BEAMS BY CONTINUOUS WAVELET TRANSFORM

Lorenzo MONTANARI[1], Andrea SPAGNOLI[*1], Biswajit BASU[2], and Brian BRODERICK[2]

[1]Department of Civil-Environmental Engineering and Architecture, University of Parma, Viale Usberti 181/A, 43124 Parma, Italy

[2]Department of Civil, Structural and Environmental Engineering, Trinity College, Dublin 2, Ireland

ABSTRACT. ~~As the ability of M~~modern measurement techniques are improving in capability to capture spatial displacement fields occurring in deformed structures with high precision and in a quasi-continuous manner. ~~the spatial displacement fields occurring in deformed structures,~~ This in turn has made the use of vibration-based damage identification methods ~~is becoming more and~~ more effective and reliable for real applications. However, practical measurement and data processing issues still ~~re~~represent barriers to the application of these methods in identifying several types of ~~for many forms of~~ structural damage. Th~~is~~e ~~present~~ paper deals with ~~the~~ spatial Continuous Wavelet Transform (CWT) damage identification method~~s~~ in beam structures with the aim of addressing ~~answering to~~ the following key questions: (i) can the cost of damage detection be reduced by down-sampling? (ii) what is the minimum number of sampling intervals required for ~~the~~ optimal damage detection ? The first three free vibration modes~~s~~ of a cantilever and a simple supported beam with an edge open crack are numerically simulated. A thorough parametric study is carried out by taking into account the key parameters governing the problem, including the wavelet mother function, level of ~~data~~ noise, crack depth and location, mechanical and geometrical ~~beam~~ parameters of the beam and the use of a padding method to reduce border distortions. The results are employed to assess the optimal number of sampling intervals for effective damage detection.

*Corresponding author: spagnoli@unipr.it

KEYWORDS: spatial sampling interval; down-sampling; vibration-based damage identification; wavelet analysis; CWT; padding method; cracked beam.

1. INTRODUCTION

Thanks to the~~ir~~ multi-resolution properties, wavelet~~s~~ functions act as a microscope with the ability to analyze the details of non-stationary signals and to localize their singularities or those of their derivatives [1]. In the past decades, Continuous Wavelet Transform (CWT) has widely been recognized to be an effective and powerful tool for identifying the damage in Structural Health Monitoring (SHM) by analyzing static or dynamic structural response in the spatial~~ce~~ domain [2].

Liew and Wang [3] and Wang and Deng [4] ~~first~~ analysed ~~in the space domain by Wavelet Transform (WT), the~~ numerical and experimental, static and dynamic, structural responses of simple cracked beams to identify damage in the spatial domain by Wavelet Transform (WT). They highlighted that Wavelet Analysis (WA) is capable of identifying the abrupt variation in beam deflection due to damage through a local abnormality of the wavelet coefficients at that position. Subsequently several authors have examined in-depth the vibration-based damage identification by wavelet analysis and applied~~y~~ it to a variety of structural problems showing its effectiveness and versatility.

Focusing on the Gaussian wavelets, Gentile and Messina [5] discuss in a numerical-theoretical way the CWT features of derivation, convolution and smoothing of noisy data. Due to the limitation of the CWT in the presence of noise (CWT behaves as a high-pass filter at the fine scales and loses details at the large scales), they underline the need of a trade-off between these scales in detecting damage. Moreover, due to CWT redundancy regarding the free choice of the scale, the authors recommend the use of CWT instead of discrete wavelet transform. By analysing modeshapes of different cracked beams ~~modeshapes~~~~mode shapes~~, the authors observe that the sensitivity in damage detection with respect to crack location depends on the local curvature of the ~~modeshape~~mode shape in the damaged area. Furthermore, ~~in Ref. [6],~~ Messina [6],~~ dealing with transversal beam

vibrations in both the non-transformed and Fourier transformed domains, discuss the ability of CWT in conjunction with differential operators to act as a frequency filter and therefore to reduce undesired high frequency noise.

Pakrashi et al. in Ref. [7] present a statistical study on the identification of the existence, location, and extent of an open crack from the first fundamental ~~modeshape~~mode shape of a simply supported beam by using CWT with the 4th order Coiflet wavelet ('Coif4'). The problem of false alarm and its significant reduction by the use of multiple measurements are illustrated. Loutridis et al. [8] analyse through CWT both the analytical and the experimental fundamental vibration mode of a double-cracked cantilever beam by using the 4th order Symlet wavelet ('Sym4'). In addition to the task of locating the crack positions, they propose an intensity factor as an indicator of the crack size. Rucka and Wilde [9] analyse numerically and experimentally the first ~~modeshape~~mode-shape of a plexiglass cracked cantilever by the one-dimensional CWT and the first ~~modeshape~~mode-shape of a clamped steel plate with a central defect by the two-dimensional CWT. The Gaussian wavelet of order 4, 'Gaus4', and the reverse biorthogonal wavelet 'Rbio5.5', having both four vanishing moments, are used to analyse the beam and the plate, respectively. Through a numerical and experimental study Wang and Wu [10] detect the location of a delamination in a beam structure under static loading with a spatial wavelet transform using the Gabor wavelet. A barely visible perturbation in the deflection profile of the delaminated beam at the two delamination edges owing to the curvature discontinuity is discerned through the WA.

In order to successfully identify damage through spatial wavelet analysis, precise and spatially dense monitored data are necessary. In the last decades, a number of researchers have focused on developing replacements for traditional sensors (e.g. accelerometers, strain gages, load cells), which have the limitation of measuring the relevant parameters at a single location and of requiring cumbersome wiring. The modern measurement techniques, on the other hand, can capture the spatial field of the relevant parameters with high precision and in a quasi-continuous manner, even

for large civil engineering structures. Such techniques include the Digital Imagine Correlation (DIC) and the digital imagine stereo-correlation (3D-DIC) [11-13], Global Positioning Systems (GPS) [14-15], Local Positioning Systems (LPS) [16-17], scanning laser vibrometers [18-19] and optic fiber sensors [20-21].

In order to fully exploit the potential~~ity~~ and versatility of the spatial wavelet analysis when quasi-continuous spatial measurement data are available, the present investigation is centered on the impact of the spatial sampling of beam deflection shapes in detecting damage. The state of the art highlights that in vibration-based damage detection methods the issue of selecting an appropriate sampling interval to discretize operational deflection shapes is well known, but few authors have investigated it in-depth.

Sazonov and Klinkhachorn [22] provide analytical and numerical arguments to select the optimal ~~modeshape~~mode ~~-~~shape sampling interval to maximize sensitivity to damage and accuracy of damage localization. They highlight that the effects of measurement noise invalidate the intuitively reasonable idea that smaller sampling intervals mean higher precision in damage localization. Guan and Karbhari [23], noticing that modal curvature methods exhibit problems related to large sampling intervals and that measurement noise increase with numerical differentiation procedures, propose a new damage identification method based on the concept of element modal strain damage index which is able to correctly locate a damage region even using sparse measurements of noisy data. Zhong and Oyadiji [24] analyze the sampling interval sensitivity for damage detection in simply supported cracked beams using three different methods based on the Stationary Wavelet Transform (SWT). They search for the proper sampling distance as a function of depth, width and location of the crack as well as of the amount of noise. The proposed methods are shown to be robust if higher ~~modeshapes~~mode shapes are considered and to be accurate if the sampling interval with respect to the beam length is equal or less than 0.01. In Refs [25-26], Surace et al. deal with the problem of crack localization in post-damage operational beam shapes through a method based on a

polynomial annihilation technique. Through numerical simulations, they quantify the number of sampling points (19 to 100 sampling points are considered) needed for damage detection. Whilst in absence of noise, even with few measurements points (e.g. 25 data points), a small-medium crack can be located, with increased noise level cracks can be identified only by using smaller sampling intervals. Many authors [9, 27-28] observenotice that in the presence of course sampling intervals, damage detection may encounter difficulties when CWT is used. To overcome the problem, they adopt the technique of over-sampling the measured data through a cubic spline interpolation.

The present paper addresses the spatial CWT based damage identification in beam structures with the aim of answering the following key questions: (i) can the cost of damage detection be reduced by down-sampling? (ii) what is the minimum number of sampling intervals required for optimal damage detection? The first three free vibration modes of cantilever and simple supported beams with an open edge crack are considered (note that this study focuses on beams of constant cross-section, characterized by homogeneous isotropic material and linear elastic behaviour). An in-depth investigation of the effect of the spatial sampling of the beam modeshapesmode shapes in identifying the damage through the spatial CWT is carried out with reference to the minimum detectable crack. The relevant aspects parameters of the problem, such as the padding methods to reduce border distortions [29-31], the mother wavelet functions (i.e. Coiflet and Gaussian of order 4, Daubechies of order 2 and real Morlet [32]), the crack depth and its location along the beam, the level of noise (simulated by synthetic Gaussian white noise) and the mechanical and geometrical beam parameters, are identified and are made to vary. The results are thoroughly discussed in detail and the optimal number of sampling intervals for an effective damage detection is assessed.

2. MODELLING OF THE CRACKED BEAM

A cracked Euler-Bernoulli beam characterized by an open edge crack under different boundary conditions at the two ends, i.e. clamped-free (cantilever beam) and supported-supported (simply

supported beam), is considered (Fig. 1). The free vibration responses are analytically evaluated by solving the free vibration equations of the two uncracked sub-beams connected by a rotational spring (representing the local stiffness k_c of the cracked cross-section of the beam) at the crack location x_c. The beam has a rectangular cross-section with height h and width b; the crack depth is a and L is the beam length. The symbols I, A, E and ρ represent, respectively, moment of inertia and area of the cross-section and Young's modulus and density of the material.

Fig. 1 - Sketch of the two cracked beams under study.

The free vibration equation related to the two uncracked parts of the beam can be written as

$$EI\frac{\partial^4 v(x,t)}{\partial x^4}+\rho A\frac{\partial^2 v(x,t)}{\partial t^2}=0\,, \tag{1}$$

where $v(x, t)$ is the transversal displacement of the beam from its static equilibrium position at a distance x from the left end at the time t. Separating the variables in Eq. (1) ($v(x,t)=\eta(x)\,g(t)$) and solving the characteristic equation function of x, the ~~modeshapes~~mode-shapes η_L and η_R of the left and right sub-beam, respectively, are as follows

$$\eta_L = C_{1L}sen(\alpha x)+C_{2L}\cos(\alpha x)+C_{3L}senh(\alpha x)+C_{4L}\cosh(\alpha x) \quad 0\le x\le x_c \tag{2.1}$$

and

$$\eta_R = C_{1R}sen(\alpha x)+C_{2R}\cos(\alpha x)+C_{3R}senh(\alpha x)+C_{4R}\cosh(\alpha x) \quad x_c\le x\le L\,, \tag{2.2}$$

where $\alpha=\left(\frac{\rho A\omega^2}{EI}\right)^{1/4}$ and ω is the natural frequency of the cracked beam.

The $C_{(.)}$ terms are integration constants arising from the solution of the fourth order differential equation in space. By imposing the boundary conditions (see Eqs 3 below), a system of eight linear equations is formed. The natural frequencies of the cracked beam are found by setting the

determinant of the matrix of the linear system to zero and solving it numerically for the roots of α. The coefficient C_{1L} is imposed to be equal to unity.

The boundary conditions of the cantilever beam at the clamped and at the free end are, respectively:

$$\eta_L(0) = 0 \quad \text{and} \quad \eta_L'(0) = 0\,, \tag{3.1}$$

$$\eta_R''(L) = 0 \quad \text{and} \quad \eta_R'''(L) = 0\,. \tag{3.2}$$

The boundary conditions of the simple supported beam at the two ends are:

$$\eta_L(0) = 0 \quad \text{and} \quad \eta_L''(0) = 0\,, \tag{3.3}$$

$$\eta_R(L) = 0 \quad \text{and} \quad \eta_R''(L) = 0\,. \tag{3.4}$$

For both the beams, the conditions of continuity of displacement, moment and shear at the crack location can be expressed as

$$\eta_L(x_c) = \eta_R(x_c)\,, \quad \eta_L''(x_c) = \eta_R''(x_c) \quad \text{and} \quad \eta_L'''(x_c) = \eta_R'''(x_c)\,. \tag{3.5}$$

The rotational spring at the cracked section introduces a discontinuity of the rotation which can be written as

$$\eta_R'(x_c) - \eta_L'(x_c) = \frac{EI}{k_c}\eta_R''(x_c)\,. \tag{3.6}$$

The local stiffness k_c is evaluated, according to linear elastic fracture mechanics concepts, through the following ~~polynomial~~ expression [33]

$$k_c = \frac{bh^2E}{24(\delta/(1-\delta))^2(5.93-19.69\delta+37.14\delta^2-35.84\delta^3+13.12\delta^4)}\,, \tag{4}$$

where $\delta = a/h$ is the relative crack depth.

Formatted Table

3. DAMAGE DETECTION BY SPATIAL CWT

3.1. Wavelet Analysis

DueThanks to its multi-resolution properties, wavelet analysis, acting as a signal microscope, appears to have a better ability to analyze the details of non-stationary signals in comparison to traditional analysis tools, such as Fourier Transform or Short-Time Fourier Transform.

A wavelet function $\psi(x)$ is a zero mean local wave-like function which decays rapidly and satisfies particular conditions [1]. A family of wavelet functions can be obtained by considering:

$$\psi_{k,s}(x) = \frac{1}{\sqrt{s}}\psi\left(\frac{x-k}{s}\right), \tag{5}$$

where s and k are, respectively, the scale and the translation parameter. The continuous wavelet transform of a signal $\eta(x)$ with respect to the wavelet function $\psi(x)$ is defined as

$$W(k,s) = \int_{-\infty}^{+\infty} \eta(x)\frac{1}{\sqrt{s}}\psi^*\left(\frac{x-k}{s}\right)dx \tag{6}$$

where ψ^* is the complex conjugate of ψ.

Since the identification of a discontinuity in a function or in any of its derivatives can be linked to the number of vanishing moments of the analyzing wavelet function (e.g. see Ref. [34]), it is possible for a wavelet transform to detect singularities by choosing an appropriate basis function $\psi(x)$. Since the presence of an open crack in a beam may introduce a singularity in the derivatives of the deflected shape, wavelet transform is deemed to be a powerful tool to locate the damage. Due to the presence of the singularity, a wavelet transformed deflected shape yields a local variation or extremum of the wavelet coefficient at the location of damage throughout the different scales.

In the present study different wavelet functions, i.e. the 4th order Coiflets wavelet ('Coif4'), with 8 vanishing moments, the 2nd order Daubechies wavelet ('Db2') with 2 vanishing moments, the 4th order Gaussian wavelet ('Gaus4') with 4 vanishing moments, and the real Morlet wavelet ('Morl') [32], are used in the CWT in order to enlarge the investigation of the impact of the sampling interval in damage detection. Furthermore, a MATLAB routine to perform the CWT for the aforementioned wavelets is implemented by the authors to improve the accuracy of the existing

built-in one (the original routine approximates the signal through a constant piecewise function, while the implemented one considers a linear piecewise trend) [35].

3.2. Noisy data simulation

Realistic situations are simulated in the following by superimposing noise to the signal corresponding to the beam deflection obtained from the mechanical model described in Section 2. It should be borne in mind that, in the ideal situation of no noise, wavelet analysis would actually be unnecessary to detect the damage position, since by numerically calculating the second derivative of the original signal the damage location can promptly be identified [36].

The presence of noise is simulated by adding a synthetic Gaussian white noise to the original response. To quantify the noise level, the signal to noise ratio (SNR) is considered. The SNR, expressed in decibels, is defined as

$$SNR = 10\log_{10}\left(\frac{P_{signal}}{P_{noise}}\right). \tag{7}$$

The term P with the subscripts in Eq. (7) denotes power and is computed as

$$P_{(.)} = \frac{1}{N_z}\sum_{i=1}^{N_z}\left|z(x_i)\right|^2, \tag{8}$$

where N_z denotes the number of discrete points of a generic sampled function $z(x)$.

3.3. Padding methods to reduce CWT edge effects

As above-mentioned, the CWT is defined by the convolution of the input signal $\eta(x)$ with a wavelet function generated by scaling and translating its mother wavelet $\psi(x)$. For a finite-length signal, when the convolution operation is executed close to the signal ends, the wavelet window extends into a region with no available data, so that the transform values close to the borders of the signal are tainted by the nonexistence of data. Consequently, the values of the CWT coefficients

very close to the signal extrema arise abnormally (border distortions) and the real signal features of that region are consequently corrupted by the transform. As a result, edge effects can provoke the masking of the damage and yield false indicators.

To handle edge effects three extrema extension methods are considered in the following:

(i) the traditional linear padding method [29], which applies a linear extension, interpolating the first two and last two values of the beam deflection shape (Fig. 2a);

(ii) the isomorphism padding methods proposed by Messina [30], which extend the signal either through a polar-like symmetry (called "Rotation") when its second derivative tends to zero or a mirror symmetry (called "Turnover") when its first derivative tends to zero (Fig. 2b);

(iii) the polynomial extension method suggested by Montanari et al. [31], which pads the original signal by means of two high degree polynomial functions obtained through a fitting procedure. The extension functions satisfy continuity conditions and extend the trend of the noisy signal and its derivatives in an average sense (Fig. 2c).

Fig. 2 - A generic noisy data signal, $\eta(x)$, is extended through: (a) linear padding method [29], (b) isomorphism padding methods proposed by Messina [30]; (c) polynomial extension method proposed by Montanari et al. [31].

4. PARAMETRIC STUDY

The effect of the sampling interval of the cracked beam ~~modeshape~~mode ~~-~~shape in damage detection through the spatial CWT is numerically analysed varying the relevant parameters of the problem, that is: the normalized sampling interval ~~*dx*~~$\Delta x/L$ ~~(*dx*~~($\Delta x/L$ is considered equal to 0.025, 0.01, 0.005, 0.0025, 0.001, 0.0005 and 0.00025), the noise level (SNR value is assumed equal to 130 dB, 100 dB or 70 dB), the padding method (see Section 3.3), the wavelet function (i.e. 'Coif4',

'Db2', 'Gaus4' and 'Morl'), the deformed shape of the beam (i.e. the first three ~~modeshapes~~mode shapes of the cantilever and of the simply supported beam) and the relative crack position along the beam (x_c/L is considered equal to 0.1, 0.3, 0.5, 0.7 or 0.9).

In this Section, a cracked beam of length L = 1 m with a rectangular cross-section of height h = 0.05L and width b = 0.5h, constituted by an elastic linear isotropic material of Young modulus E = 200 GPa and density ρ = 7850 kg/m^3, is considered. In Section 5, the influence of the beam parameters on the effect of the sampling interval in detecting the damage is analyzed. Note that, for the present 1m-long beam, normalized sampling intervals of 0.001, 0.0005 and 0.00025 would yield unrealistic distances between measurement points, but they are considered in the following simulations in order to explore a broad range of sampling intervals.

4.1. Criterion for minimum detectable crack size

In order to investigate the effect of sampling interval in CWT based damage detection, the minimum detectable (threshold) crack size for a given spatial sampling interval is obtained according to the following criterion based on an iterative procedure.

While increasing gradually the relative crack depth δ from a value of 0.0001 to 0.95, the wavelet transform is executed at fixed values of the scale s ($s = 2,4,6,\ldots,200$) and the maximum absolute value of the transform is determined for each scale. If for a given relative crack depth δ this maximum is attained for all scales at the crack position for each of an arbitrary number of 20 different random Gaussian white noise distributions, this value of δ can be regarded to be detectable, otherwise a larger value of δ has to be assessed. To allow for the numerical approximation of the CWT, the crack depth is also regarded as detectable even if the CWT absolute maximum is attained in either of the two nearest points (i.e. the preceding or the following point) to the actual damage location. For very small sampling intervals ($\Delta x/L < 0.005$), the criterion is relaxed to any of the four nearest points to the damage location.

The results pertaining to the effect of sampling interval on the minimum detectable crack size are presented in the following Sections (see the bilogarithmic graphs in Figs 3-9) as a function of the pseudo-frequency, $f_a = f_c/(\Delta x \cdot s)$, where f_c is the center frequency of the mother wavelet (i.e. the frequency maximizing the Fourier transform of the mother wavelet modulus~~; the~~ [29]). The values of center frequency f_c for the considered mother wavelets are: 0.6957 for 'Coif4', 0.6667 for 'Db2', 0.318 for 'Gaus4' and 0.8125 for 'Morl'~~).~~.

4.2. Sampling effect varying the padding method

~~Firstly t~~The present study deals with the effect of sampling interval on CWT near-edge crack detection (x_c/L = 0.1 is considered) using different padding methods (linear, Messina's and polynomial padding methods are analysed). The first ~~modeshape~~mode-shape of the cantilever beam is investigated and the 'Coif4' wavelet is used in the CWT.

Figures 3, 5 and 6 represent, for different noise levels and padding methods, the minimum detectable relative crack depth δ as a function of the data relative sampling distance ~~dx~~$\Delta x/L$ and of the pseudo-frequency f_a. Graphs (a) refer to 'low' noise (SNR = 130 dB), graphs (b) to 'intermediate' noise (SNR = 100 dB) and graphs (c) to 'high' noise (SNR = 70). Note that the curves in Figs 3, 5 and 6 are plotted by considering an upper limit of δ equal to 0.95.

By juxtaposing the results reported in Figs 3, 5 and 6, it can be observed that the padding method significantly influences the relation between minimum detectable crack size and pseudo-frequency. When the linear padding method is used, considering $f_a \geq 12$ m^{-1}, at low noise level (SNR = 130 dB) the damage identification is a function of the pseudo-frequency only and not of the sampling interval (Fig. 3a). At higher noise levels, at a given value of pseudo-frequency larger sampling intervals are observed to be more effective in damage detection (see Figs 3(b,c)). This occurrence is attributable to be due to the linear extension method whose performance in reducing edge effects can decrease substantially in the presence of high noise and very small sampling step.

Moreover, considering $f_a \geq 12$ m^{-1}, the curves in Fig. 3 present a positive curvature with a minimum value, regardless of the sampling distance, at about the same pseudo-frequency equal to around 330, 60 and 12 m^{-1} for SNR equal to 130, 100 and 70 dB, respectively (note that in Figs 3(b-c) for very low values of ~~*dx*~~*Δx*/*L* the positive curvature is not evident). This behavioral trend is caused by two reasons: the noise influence and the edge effects due to the linear padding. Moving from the high to low values of f_a, since high values of f_a are very sensible to noise, smaller cracks can only be detected until a minimum detectable crack size for certain level of noise is reached (the part of the curves to the right of the minimum value is ruled by the *presence of noise*). When decreasing beyond a certain value f_a, the wavelet detects the edge discontinuity due to the padding method (the part of the curves to the left of the minimum value is ruled by the *edge effects*).

Finally, as expected, the minimum detectable crack size tends to decrease with decreasing noise level.

Fig. 3 – Impact of the sampling interval in damage detection by spatial CWT with 'Coif4'. The linear padding method is used. The first ~~modeshape~~mode-shape of the cantilever beam with crack at x_c/L = 0.1 is analysed. (a) SNR = 130 dB; (b) SNR = 100 dB; (c) SNR = 70 dB.

At this point it might be worth explaining the reasons why for $f_a < 12$ m^{-1} the curves of Fig. 3 deviate from the behavioral trend described above, showing a vertical asymptote corresponding to about $f_a = 2.4$ m^{-1}. These reasons are related to the treatment of the edge effect at x = 0 using the linear padding method and the crack location close to that beam end (x_c/L = 0.1), as discussed in the following.

When the linear padding method is applied to a signal end with curvature different from zero (at x = 0 in the case of the cantilever 1st ~~modeshape~~mode-shape), the second derivative of the padded signal presents a severe discontinuity at that position [31]. Consequently, as shown in Fig. 4, the

CWT analysis of the padded beam shape exhibits, when δ is smaller than a certain value, the highest coefficients close to the clamped end of the beam. For instance, using s = 8, corresponding to f_a = 17.4 m^{-1}, the highest value of the wavelet coefficients is at $x/L \cong 0.02$ when $\delta \leq 0.05$, while using s = 52, corresponding to f_a = 2.7 m^{-1}, it is at $x/L = 0.1$, regardless of the value of δ (the blue curves related to δ = 0 in Fig. 4b are overlapped by the green and red ones). This means that, around the pseudo-frequency range $f_a = [2-4]$ m^{-1}, the CWT analysis does not detect the presence of tiny cracks but the discontinuity due to the linear padded method at x = 0 (Fig. 4b) and the vertical asymptotic trend of Fig. 3 takes place. On the other hand, as shown in Fig. 4a, by analyzing the signal by means of high pseudo-frequencies (f_a = 17.4 m^{-1} is used), for small crack sizes the wavelet analysis is more sensitive to the discontinuity due to the padding method, while for large crack size, the wavelet analysis is more sensitive to the crack discontinuity and the damage identification is satisfied. Analogous reasoning can be made for f_a smaller than about 1.3 m^{-1}.

Fig. 4 – Zoom of the normalized absolute values of the CWT coefficients obtained by analyzing the normalized first ~~modeshape~~mode-shape of the cantilever beam with crack at x_c/L = 0.1 varying the relative crack depth δ. The signals are sampled at ~~dx~~$\Delta x/L$ = 0.005, considering SNR = 100 dB. Two different scales are considered: (a) s = 8, corresponding to f_a = 17.4 m^{-1} in Fig. 3; (b) s = 52, corresponding to f_a = 2.7 m^{-1} in Fig. 3.

In contrast to the results obtained with the linear padding method, when applying Messina's padding method, regardless of the noise level, the CWT- f_a curves for different values of ~~dx~~$\Delta x/L$ tend to overlap and the damage identification becomes, with good approximation, a function of the pseudo-frequency only (see Fig. 5). This implies that, since the scale can be made to vary as desired, large sampling intervals can be as effective as small ones. As for linear padding with decreasing noise level, smaller cracks can be detected.

As in Fig. 3, the curves of Fig. 5 present a positive curvature with a minimum value, but now, given the smaller influence of border discontinuities on the CWT introduced by Messina's padding method [31], the curves of Fig. 5 attain their minimum value at a lower pseudo-frequency than that observed in Fig. 3. The values of pseudo-frequency offering optimal damage detection are equal to around 45, 16 and 5 m^{-1} for SNR values equal to 130, 100 and 70 dB, respectively.

Fig. 5 – Impact of the sampling interval in damage detection by spatial CWT with 'Coif4'. Messina's padding method is used. The first ~~modeshape~~mode-shape of the cantilever beam with crack at x_c/L = 0.1 is analysed. (a) SNR = 130 dB; (b) SNR = 100 dB; (c) SNR = 70 dB.

By using the polynomial padding method [31], ~~(the following parameters are assumed, $\beta_1 = \beta_2 = 1$, $H_1 = \overline{H}_1$, $H_2 = \overline{H}_2$)~~ the damage identification turns out to be, with good approximation, a function of the pseudo-frequency only (~~Fig. 6).~~in the simulations of Fig. 6 the fitting parameters of the method are assumed to be $\beta_1 = \beta_2 = 1$, $H_1 = \overline{H}_1$ and $H_2 = \overline{H}_2$). However the curves of Fig. 6 exhibit a different trend than those obtained with the linear and Messina's padding methods. Rather than being characterized by a positive curvature, they decrease monotonically from high to low pseudo-frequencies until, at a specific frequency, a sudden jump occurs toward the upper limit of δ (say, equal to 0.95). This specific value of pseudo-frequency represents, with good approximation, the *lowest* and *optimal* value of pseudo-frequency for damage identification (the optimal value is that allowing the minimum crack size to be detected as the pseudo-frequency is made to vary). It needs to be underlined that this lowest/optimal value of f_a is the same for all levels of noise. As shown further in Section 4.3, this result appears to occur when the polynomial padding method is used together with wavelet functions characterized by many vanishing moments.

The jump in the curves of Fig. 6 at the lowest/optimal value of f_a occurs because, by analyzing the cracked beam shape with wavelet functions characterized by lower pseudo-frequencies, even large cracks cannot be localized due to the influence of the edge effects. In Section 4.5 it will be illustrated that lower pseudo-frequencies can detect cracks located further away from the beam end, but in any case below a certain value of f_a, damage detection fails due to the edge effects even in the presence of large cracks.

Figure 6 shows that the curves for ~~dx~~$\Delta x/L$ = 0.00025 exhibit jumps to the upper limit of δ at a higher value of pseudo-frequency than those for larger sampling intervals. This trend is due to the fact that, when the crack is near the signal extremum, the wavelet analysis is tainted by edge distortions, and, particularly for very low sampling intervals, the maximum CWT coefficient value falls not exactly at the crack location (or at its two four nearest points, as permitted by the detection criterion), but at sampling points other from that of the crack location. In Section 4.5, it will be shown that when the crack is located far away from the beam ends, regardless of the value of the sampling interval, the lower bound of pseudo-frequency is the same.

Hereafter, due to its effectiveness and versatility in handling general shapes of beam deflection [31], the polynomial padding method is used and, since the minimum detectable crack size is effectively only f_a dependent, the results are shown as a function of the noise level only, irrespectively of the sampling interval. Note that, in order to reduce the computational cost, $H_1 = \overline{H}_1$ and $H_2 = \overline{H}_2$ is always imposed, but this assumption does not affect the results of this investigation.

The $f_{a,opt}$ is used to indicate the optimal value of pseudo-frequency f_a that gives the minimum detectable crack size ($f_{a,opt}$ is equal to about 12 m^{-1} in Fig. 6). The value $f_{a,opt}$ of pseudo-frequency approximately coincides, as shown above, with the lowest pseudo-frequency for performing damage detection.

Fig. 6 – Impact of the sampling interval in damage detection by spatial CWT with 'Coif4'. The polynomial padding method is used. The first ~~modeshape~~mode ~~-~~shape of the cantilever beam with crack at x_c/L = 0.1 is analysed. (a) SNR = 130 dB; (b) SNR = 100 dB; (c) SNR = 70 dB.

4.3. Sampling effect varying the wavelet function

Figure 7 displays the results of the sampling step impact in the CWT damage detection executed using the 2nd order Daubechies ('Db2'), the 4th order Gaussian ('Gaus4') and the Morlet ('Morl') wavelet functions. The first ~~modeshape~~mode shape of the cantilever beam with crack at x_c/L = 0.1 is analysed.

Figure 7a shows that CWT damage identification by 'Db2', conversely to that by the other wavelet functions, depends on both ~~'dx'~~ '$\Delta x/L$' and f_a. In addition, 'Db2' exhibits a poor damage identification performance due to its characteristic of having only two vanishing moments [34]. Similarly to 'Coif4', using 'Gaus4' and 'Morl', the damage detection is, with good approximation, just pseudo-frequency f_a dependent in the medium-high f_a range. In particular, using 'Morl' the lower limit of f_a (corresponding to large values of ~~'dx'~~ '$\Delta x/L$') appears to be the smallest among those of the wavelet functions considered. The behavioral trend of results shown in Fig. 7 seems to be similar for the different SNR values considered.

The comparison with the results for 'Coif4' (see Fig. 6) demonstrates that 'Coif4' exhibit the best performances in damage detection in comparison to the other wavelet functions, and hence it is adopted throughout in the following.

Fig. 7 – Impact of the sampling interval in damage detection by spatial CWT varying the wavelet function. The polynomial padding method is used and the first ~~modeshape~~mode ~~-~~shape of the

cantilever beam with crack at x_c/L = 0.1 is analysed. (a) 'Db2'; (b) 'Gaus4'; (c) 'Morl'.

4.4. Sampling effect varying the ~~modeshape~~mode-shape

The second and the third ~~modeshapes~~mode shapes of the cantilever beam and the first three ~~modeshapes~~mode shapes of the simply supported beam are now analysed. The crack is located at x_c/L = 0.1. Figure 8 illustrates the effect of the sampling interval in CWT damage detection using 'Coif4' and the polynomial padding method ($\beta_1 = \beta_2 = 1$ is used in Figs 8(a,c), $\beta_1 = 0.25$ and $\beta_2 = 0.33$ in Fig. 8b, $\beta_1 = \beta_2 = 0.5$ in Fig. 8d and $\beta_1 = \beta_2 = 0.3$ in Fig. 8e). The jumps in the curves at low frequencies are dependent on the analysed ~~modeshape~~mode-shape but, neglecting this disturbance due to edge effects, damage identification appears to be a function of f_a only. In Figs 8(a-e) the optimal pseudo-frequency $f_{a,opt}$ is, respectively, equal to about 11 m^{-1}, 18 m^{-1}, 12 m^{-1}, 16 m^{-1} and 21 m^{-1}.

Fig. 8 – Impact of the sampling interval in damage detection by spatial CWT with 'Coif4'. The polynomial padding method is used and different beam ~~modeshapes~~mode-shapes with the crack at x_c/L = 0.1 are analysed. (a,b) second and third ~~modeshape~~mode-shape of the cantilever beam, respectively; (c,d,e) first, second and third ~~modeshape~~mode-shape of the simply supported beam, respectively.

4.5. Sampling effect for various crack locations

The effect of the sampling interval in the CWT damage detection is further investigated by varying the crack location: x_c/L = 0.3, 0.5, 0.7 and 0.9 are considered. The first ~~modeshape~~mode shape of the cracked cantilever beam is analysed. By juxtaposing the results of Fig. 9 with those reported in Figs 3 to 8, the influence of border distortions in dictating the optimal value $f_{a,opt}$ of pseudo-frequency of the curves is clearly manifested. The further the crack location is from either

beam end, the lower is the optimal pseudo-frequency $f_{a,opt}$. This means that damage detection can be achieved with a reduced number of sampling points. Furthermore, Figs 9(a-c) show that, since the crack is far away from the beam ends, the $f_{a,opt}$ is the same for each curve. In contrast in Fig. 9d, since the crack is close to the beam end (i.e. x_c/L = 0.9), a similar trend to that of Fig. 6d is shown. In Figs 9(a-d) the optimal pseudo-frequency $f_{a,opt}$ is, respectively, equal to about 6 m^{-1}, 2.5 m^{-1}, 6 m^{-1} and 12 m^{-1}.

Fig. 9 – Impact of the sampling interval in damage detection by spatial CWT with 'Coif4'. The polynomial padding method is used; The first ~~modeshape~~mode-shape of the cantilever beam with a crack at different locations is analysed. (a) x_c/L=0.3; (b) x_c/L=0.5; (c) x_c/L=0.7; (d) x_c/L=0.9.

4.6. Discussion of the results

Focusing on the results of Sections 4.2 – 4.5, pertaining to the use of the polynomial padding method and the 'Coif4' wavelet, the following conclusions can be drawn:

(i) there is an optimal value of pseudo-frequency, independent of the noise level, which maximizes the performance of the damage detection for a given beam deflection shape and crack position;

(ii) by adjusting the wavelet scale, damage detection performances can be similar for small and large sampling intervals.

Considering that CWT based damage detection ~~can be considered to~~ depends on the pseudo-frequency only, it is numerically illustrated how the use of the proper scale range is essential in detecting damage when different sampling intervals are considered [31].

The first ~~modeshape~~mode-shape of the cantilever beam, defined at the beginning of Section 4, with a crack of δ = 0.2 at x_c/L = 0.1 is analysed. The noise level is assumed to be equal to 70 dB. The same ~~modeshape~~mode-shape is sampled at ~~dx~~$\Delta x/L$ = 0.01 and ~~dx~~$\Delta x/L$ = 0.0004.

Figs 10(a,b) report the contour plots of the CWT ('Coif4' and the polynomial padding method with $\beta_1 = \beta_2 = 1$ are used) when the signal is sampled at ~~dx~~$\Delta x/L$ = 0.01, and the scale ranges $s = [4-24]$ (i.e. $s = 4, 5, 6\ldots, 24$) and $s = [4-6]$ are respectively used. The CWT coefficients, considering the broad scale range, completely mask the crack location (Fig. 10a), which on the contrary can be identified using the narrow scale range (Fig. 10b).

Figures 10(c-d) highlight that even if the signal is sampled at an extremely small sampling interval (~~dx~~($\Delta x/L$ = 0.0004), the CWT damage detection can be achieved only considering a proper scale range. The damage localization at the scale range $s = [2-40]$ fails (Fig. 10c), while it succeeds for $s = [96-158]$ (Fig. 10d).

The results reported in Fig. 10 are in agreement with those of Fig. 6c, which deal with the same beam deflection. Indeed Fig. 6c highlights that the optimal pseudo-frequency is in the range $f_a = [11-18]$ m^{-1}, which for ~~dx~~$\Delta x/L$ = 0.01 corresponds to the scale range $s = [4-6]$, and for ~~dx~~$\Delta x/L$ = 0.0004 to $s = [96-158]$.

Fig. 10 – Contour plots of the spatial CWT using 'Coif4' and the polynomial padding method (SNR = 70 dB). The first ~~modeshape~~mode-shape of the cantilever beam with crack of δ = 0.2 at x_c/L = 0.1 is analysed. Sampling interval ~~dx~~$\Delta x/L$ and scale range are varied: (a) ~~dx~~$\Delta x/L$ = 0.01, $s = [4-24]$; (b) ~~dx~~$\Delta x/L$ = 0.01, $s = [4-6]$; (c) ~~dx~~$\Delta x/L$ = 0.0004, $s = [2-40]$; (d) ~~dx~~$\Delta x/L$ = 0.0004, $s = [96-158]$.

5. GENERALIZATION OF THE RESULTS

The results reported in Figs 3 to 9 in terms of minimum detectable crack size are related to beams characterized by particular values of the parameters ρ, h, b, L and E. In this Section, the

influence of these beam parameters on the optimal pseudo-frequency in CWT based damage detection with the polynomial padding method and a fit wavelet function (e.g 'Coif4'), is analysed and a further generalization of the parametric study is obtained.

~~Since~~According to Eq. 2, the functions describing the general mode~~–~~shape depend on the boundary conditions and on the parameter α, and in turns the corresponding natural frequency is a function of the material density ρ and of α. Hence, the material density ρ affects the natural frequencies of the cracked beam but not its ~~modeshapes, this beam parameter turn out to be negligible~~mode shapes and it is not considered in the following.

Then, by substituting the LEFM expression of the local rotational stiffness k_c due to the crack (Eq. 4) in the boundary condition representing the rotation discontinuity at the crack section (Eq. 3.6), we obtain:

$$\eta_2'(x_c) - \eta_1'(x_c) = 2h\,\tilde{f}(\delta)\,\eta_2''(x_c)\,, \tag{9}$$

where $\tilde{f}(\delta) = (\delta/(1-\delta))^2(5.93 - 19.69\delta + 37.14\delta^2 - 35.84\delta^3 + 13.12\delta^4)$ is a function of the relative crack depth δ only. For a given beam deflection shape (and, hence, for a given value of the curvature in x_c, $\eta_1''(x_c) = \eta_2''(x_c)$), Equation 9 demonstrates that the rotation discontinuity due to the crack is a function of h and δ, but not of the other beam parameters b and E. Therefore, the CWT based damage detection results are invariant for constant values of h, ~~and~~ δ, and~~keeping~~ L, ~~constant~~, ~~the CWT damage detection capacity does not vary.~~

As for the beam parameter h, it can be demonstrated [~~31~~35] that its variation influences the detectable crack depth but not the optimal pseudo-frequency value of CWT damage detection. In summary, the optimal pseudo-frequency $f_{a,opt}$ is independent of the beam parameters b, h, E and ρ and hence, using the polynomial padding method and a given wavelet function, it is a function of the deformed beam shape and the crack position x_c. Formally, this can be written as:

$$f_{a,opt} = \mathrm{f}\,(\text{beam deflection shape}, x_c, L)\,. \tag{10}$$

Through the dimensional analysis and Buckingham's theorem [37], Eq. 10 can be expressed in the following dimensionless form:

$$f^{*}_{a,opt} = f_{a,opt} L = \text{f (beam deflection}, x_c / L), \tag{11}$$

Equation 11 states that the optimal pseudo-frequency $f_{a,opt}$ multiplied by the beam length L is a function of the beam deflection shape and the relative crack position x_c/L only.

Figure 11 illustrates the $f^{*}_{a,opt}$ against x_c/L curves pertaining to the first three ~~modeshapes~~mode shapes of the cantilever and simply supported beams. It can be noted that, mainly due to the edge effects, $f^{*}_{a,opt}$ turns out to be higher near the beam ends, especially for the third ~~modeshapes~~mode shapes.

Fig. 11 – Variation of $f^{*}_{a,opt}$ for the CWT damage detection with relative crack location for the first three ~~modeshapes~~mode-shapes of: (a) cantilever beams; (b) simply supported beams.

According to the curves of Fig. 11, for a given wavelet scale, it is possible to calculate the optimal number of sampling intervals needed to detect the smallest crack located at x_c/L using a given beam vibration ~~modeshape~~mode-shape. For example, consider the requirement to monitor the service state of a ~~wind turbine blade~~cantilever of L = ~~50~~5 m through the spatial CWT using the polynomial padding method and 'Coif4' wavelet. By analyzing the ~~blade's~~cantiliver's first ~~modeshape~~mode–shape (or operational shapes similar to the first ~~modeshape~~mode–shape), the optimum sampling interval to detect the smallest crack located more than 0.1m from the blade ends is $\Delta x = \dfrac{f_c L}{f^{*}_{a,opt} s} = \dfrac{0.6957 \cdot 50}{24 \cdot 2} \cong 0.\text{~~72~~}072$ m, for s = 2.

Finally, from the definition of $f^{*}_{a,opt}$, the optimal number of sampling intervals yielding the best CWT damage detection at the scale s for a given crack location x_c/L, is equal to:

$$\left.\frac{L}{\Delta x}\right|_{opt} = \frac{f^{*}_{a,opt}\, s}{f_c}\,. \tag{12}$$

As an example, in Fig. 12 the minimum of such an optimal number of sampling intervals is considered by taking s = 2 (the value of s = 1 is discarded in the present study) and it is plotted as a function of x_c/L.

Fig. 12 – The minimum optimal number of beam sampling intervals, L~~/dx~~/Δx, to perform the optimum CWT damage detection at scale s = 2 is plotted against the normalized crack location for the first three ~~modeshapes~~mode-shapes of: (a) cantilever beams; (b) simply supported beams.

5. CONCLUSIONS

The present investigation examined the effect of the spatial sampling interval in damage detection by CWT, with the aim of answering the following key questions: C~~c~~an the cost of damage detection be reduced by down-sampling? ~~And w~~What is the minimum number of sampling intervals required for optimal damage detection? An in-depth parametric study has been carried out by analyzing the first three ~~modeshapes~~mode shapes of a cantilever and a simply-supported beam varying the relevant parameters of the problem, that is: the sampling interval, the noise level, the padding method, the wavelet function, the crack depth and position along the beam, and the mechanical and geometrical beam parameters.

The effect of the sampling interval~~distance~~ in CWT based damage detection is investigated in terms of the minimum detectable crack size (which is defined on the basis of an ad-hoc criterion) as a function of the key parameter, pseudo-frequency. The padding method is observed to significantly influence the minimum detectable crack size. Using the linear padding method, where~~as~~ at low noise levels the damage detection is independent of the sampling interval, at medium-high noise

levels small sampling intervals appear to be less effective. On the other hand, extending the deformed beam shape through Messina's methods or the polynomial padding method, regardless of the noise level, the damage detection is independent of the sampling interval and is a function of the pseudo-frequency only. Among the different wavelet functions being analyzed, 'Coif4' seems to be the most effective.

Focusing on the findings obtained using the polynomial padding method and 'Coif4' wavelet, curves of minimum detectable crack size against pseudo-frequency for different relative sampling intervals coincide and decrease monotonically with decreasing pseudo-frequency down to a lower bound value of pseudo-frequency f_a below which no damage detection is possible. This lower bound of f_a can be regarded as the optimal pseudo-frequency $f_{a,opt}$ capable of detecting the smallest crack size by CWT. The parametric study shows that such an optimal pseudo-frequency depends on the ~~modeshape~~mode-shape and on the crack location along the beam. In addition, it has been observed ~~pointed out~~ that, for a given ~~modeshape~~mode-shape and crack position, different beam structures, characterized by the same value of x_c/L, attain the same optimal value of the dimensionless pseudo-frequency $f_{a,opt} L$.

In conclusion, even though modern measurement techniques allow beam deflection shapes to be monitored with very dense sampling points, down-sampling the measurement points reduces damage detection costs without affecting performance, as long as the optimal value of the pseudo-frequency can be achieved. The minimum optimal number of sampling intervals, corresponding to the wavelet scale equal to 2, can be determined in relation to the beam deflection shape and damage location. Finally, by performing the CWT analysis in the range of the optimal pseudo-frequency, down-sampling dense measured data can be used as a tool to verify the robustness of the results.

REFERENCES

[1] S. Mallat, A Wavelet Tour on Signal Processing, Academic Press, NewYork, 2001.

[2] Y. J. Yana, L. Cheng, Z. Y. Wua, L. H. Yam, Development in vibration-based structural damage detection technique. Mechanical Systems and Signal Processing, 21 (2007) 2198–2211.

[3] K. M. Liew, Q. Wang, Application of wavelet theory for crack identification in structures. Journal of Engineering Mechanics 124 (1998) 152–157.

[4] Q. Wang, X. Deng, Damage detection with spatial wavelets. International Journal of Solids and Structures 36 (1999) 3443–3468.

[5] A. Gentile, A. Messina, On the continuous wavelet transforms applied to discrete vibrational data for detecting open cracks in damaged beams. International Journal of Solids and Structures 40 (2003) 295–315.

[6] A. Messina, Detecting damage in beams through digital differentiator filters and continuous wavelet transforms. Journal of Sound and Vibration 272 (2004) 385–412.

[7] V. Pakrashi, B. Basu, A. O' Connor, A statistical measure for wavelet based singularity detection. Journal of Vibration and Acoustics 131(4) (2009).

[8] S. Loutridis, E. Douka, A. Trochidis, Crack identification in double cracked beams using wavelet analysis. Journal of Sound and Vibration 277(4) (2004) 1025–1039.

[9] M. Rucka, K. Wilde, Application of continuous wavelet transform in vibration based damage detection method for beams and plates. Journal of Sound and Vibration 297 (2006) 536–550.

[10] Q. Wang, N. Wu, Detecting the delamination location of a beam with a wavelet transform: an experimental study. Smart Material and Structures. 20(1) (2011) 012002.

[11] P. K. Rastogi, Optical Measurement Techniques and Applications. Artech House Inc., Boston, 1997.

[12] J.-J. Orteu, 3-D computer vision in experimental mechanics. Optics and Lasers in Engineering 47(3) (2009) 282-291.

[13] M. Ozbek, D. J. Rixen, O. Erne, G. Sanow, Feasibility of monitoring large wind turbines using photogrammetry. Energy 35(12) (2010) 4802-4811.

[14] F. Casciati, C. Fuggini, Engineering vibration monitoring by GPS: long duration records. Earthquake Engineering and Engineering Vibration 8(3) (2009) 459-467.

[15] A. Nickitopoulou, K. Protopsalti, S. Stiros, Monitoring dynamic and quasi-static deformations of large flexible engineering structures with GPS: Accuracy, limitations and promises. Engineering Structures 28(10) (2006) 1471-1482.

[16] F. Casciati, L. J. Wu, Investigating the potential of LPS in structural health monitoring. Proceedings of the Sixth International Conference on Wireless Communications Networking and Mobile Computing (WiCOM), IEEE, September 2010.

[17] F. Casciati, L. J. Wu, Global VS local positioning systems. Proceedings of the Fifth International Conference on World Conference on Structural Control and Monitoring 2010, Tokyo, July 2010.

[18] A. B. Stanbridge, D. J. Ewins, Modal testing using a scanning laser Doppler vibrometer. Mechanical Systems and Signal Processing 13(2) (1999) 255-270.

[19] S. Yang, M. S. Allen. Output-only modal analysis using continuous-scan laser Doppler vibrometry and application to a 20kW wind turbine, in: T. Proulx (Ed.), Modal Analysis Topics, vol. 3, Springer, New York, 2011, pp.47-64.

[20] H.-N. Li, D.-S. Li, G.-B. Song. Recent applications of fiber optic sensors to health monitoring in civil engineering. Engineering structures 26(11) (2004) 1647-1657.

[21] A. P. Adewuyi, Z. Wu, N. K. Serker, Assessment of vibration-based damage identification methods using displacement and distributed strain measurements. Structural Health Monitoring 8(6) (2009) 443-461.

[22] E. Sazonov, K. Powsiri, Optimal spatial sampling interval for damage detection by curvature or strain energy mode shapes. Journal of sound and vibration 285(4) (2005) 783-801.

[23] H. Guan, V. M. Karbhari, Improved damage detection method based on element modal strain damage index using sparse measurement. Journal of Sound and Vibration 309(3) (2008) 465-494.

[24] S. Zhong, S. O. Oyadiji, Sampling interval sensitivity analysis for crack detection by stationary wavelet transform. Structural Control and Health Monitoring 20(1) (2013) 45-69.

[25] C. Surace, G. Yan, R. K. Archibald, R. Saxena, R. Feng, Structural Damage Detection using the Polynomial Annihilation Edge Detection Method, Australian Journal of Structural Engineering (AJSE) 15(1) (2014), in press.

[26] C. Surace, R. Archibald, R. Saxena, On the use of the polynomial annihilation edge detection for locating cracks in beam-like structures. Computers & Structures 114 (2013) 72-83.

[27] E. Douka, S. Loutridis, A. Trochidis, Crack identification in beams using wavelet analysis, International Journal of Solid and Structures 40 (2003) 3557-3569.

[28] S. Zhong, S. O. Oyadiji, Detection of cracks in simply-supported beams by continuous wavelet transform of reconstructed modal data. Computers & structures 89(1) (2011) 127-148.

[29] M. Misiti, Y. Misiti, G. Oppenheim, J. Poggi, Wavelet Toolbox, The MathWorks Inc., 2000.

[30] A. Messina, Refinements of damage detection methods based on wavelet analysis of dynamical shapes. International Journal of Solids and Structures 45 (2008) 4068–4097.

[31] L. Montanari, B. Basu, A. Spagnoli, B. M. Broderick, A padding method to reduce edge effects for enhanced damage identification using wavelet analysis. Mechanical Systems and Signal Processing (2014), submitted.

[32] I. Daubechies, Ten lectures on wavelets, vol. 61, Society for Industrial and Applied Mathematics, Philadelphia, 1992.

[33] H. Tada, P. C. Paris, G. R. Irwin, The Stress Analysis of Crack Handbook. Del Research Corporation, St. Louis, 1985.

[34] V. Pakrashi, B. Basu, A. O'Connor. Structural damage detection and calibration using a wavelet–kurtosis technique. Engineering Structures 29 (2007) 2097-2108.

[35] L. Montanari, Vibration-based damage identification in beam structures through wavelet analysis, PhD Thesis, Univerity of Parma, 2014.

[36] A. K. Pandey, M. Biswas, M. M. Samman. Damage detection from changes in curvature mode shapes. Journal of Sound and Vibration 145(2) (1991) 321-332.

[37] H. L. Langhaar, Dimensional Analysis and Theory of Models, Wiley, New York, 1951.

Revised version, 18 November 2014

ON THE EFFECT OF SPATIAL SAMPLING IN DAMAGE DETECTION OF CRACKED BEAMS BY CONTINUOUS WAVELET TRANSFORM

Lorenzo MONTANARI[1], Andrea SPAGNOLI[*1], Biswajit BASU[2], and Brian BRODERICK[2]

[1]Department of Civil-Environmental Engineering and Architecture, University of Parma, Viale Usberti 181/A, 43124 Parma, Italy

[2]Department of Civil, Structural and Environmental Engineering, Trinity College, Dublin 2, Ireland

ABSTRACT. Modern measurement techniques are improving in capability to capture spatial displacement fields occurring in deformed structures with high precision and in a quasi-continuous manner. This in turn has made the use of vibration-based damage identification methods more effective and reliable for real applications. However, practical measurement and data processing issues still present barriers to the application of these methods in identifying several types of structural damage. This paper deals with spatial Continuous Wavelet Transform (CWT) damage identification methods in beam structures with the aim of addressing the following key questions: (i) can the cost of damage detection be reduced by down-sampling? (ii) what is the minimum number of sampling intervals required for optimal damage detection ? The first three free vibration modes of a cantilever and a simple supported beam with an edge open crack are numerically simulated. A thorough parametric study is carried out by taking into account the key parameters governing the problem, including the wavelet mother function, level of noise, crack depth and location, mechanical and geometrical parameters of the beam and the use of a padding method to reduce border distortions. The results are employed to assess the optimal number of sampling intervals for effective damage detection.

KEYWORDS: spatial sampling interval; down-sampling; vibration-based damage identification; wavelet analysis; CWT; padding method; cracked beam.

*Corresponding author: spagnoli@unipr.it

1. INTRODUCTION

Thanks to the multi-resolution properties, wavelet functions act as a microscope with the ability to analyze the details of non-stationary signals and to localize their singularities or those of their derivatives [1]. In the past decades, Continuous Wavelet Transform (CWT) has widely been recognized to be an effective and powerful tool for identifying the damage in Structural Health Monitoring (SHM) by analyzing static or dynamic structural response in the spatial domain [2].

Liew and Wang [3] and Wang and Deng [4] analysednumerical and experimental, static and dynamic, structural responses of simple cracked beams to identify damage in the spatial domain by Wavelet Transform (WT). They highlighted that Wavelet Analysis (WA) is capable of identifying the abrupt variation in beam deflection due to damage through a local abnormality of the wavelet coefficients at that position. Subsequently several authors have examined in-depth the vibration-based damage identification by wavelet analysis and applied it to a variety of structural problems showing its effectiveness and versatility.

Focusing on the Gaussian wavelets, Gentile and Messina [5] discuss in a numerical-theoretical way the CWT features of derivation, convolution and smoothing of noisy data. Due to the limitation of the CWT in the presence of noise (CWT behaves as a high-pass filter at the fine scales and loses details at the large scales), they underline the need of a trade-off between these scales in detecting damage. Moreover, due to CWT redundancy regarding the free choice of the scale, the authors recommend the use of CWT instead of discrete wavelet transform. By analysing modeshapes of different cracked beams , the authors observe that the sensitivity in damage detection with respect to crack location depends on the local curvature of the modeshape in the damaged area. Furthermore, Messina [6]dealing with transversal beam vibrations in both the non-transformed and Fourier transformed domains, discuss the ability of CWT in conjunction with differential operators to act as a frequency filter and therefore to reduce undesired high frequency noise.

Pakrashi et al. in Ref. [7] present a statistical study on the identification of the existence, location, and extent of an open crack from the first fundamental mode shape of a simply supported beam by using CWT with the 4th order Coiflet wavelet ('Coif4'). The problem of false alarm and its significant reduction by the use of multiple measurements are illustrated. Loutridis et al. [8] analyse through CWT both the analytical and the experimental fundamental vibration mode of a double-cracked cantilever beam by using the 4th order Symlet wavelet ('Sym4'). In addition to the task of locating the crack positions, they propose an intensity factor as an indicator of the crack size. Rucka and Wilde [9] analyse numerically and experimentally the first modeshape of a plexiglass cracked cantilever by the one-dimensional CWT and the first modeshape of a clamped steel plate with a central defect by the two-dimensional CWT. The Gaussian wavelet of order 4, 'Gaus4', and the reverse biorthogonal wavelet 'Rbio5.5', having both four vanishing moments, are used to analyse the beam and the plate, respectively. Through a numerical and experimental study Wang and Wu [10] detect the location of a delamination in a beam structure under static loading with a spatial wavelet transform using the Gabor wavelet. A barely visible perturbation in the deflection profile of the delaminated beam at the two delamination edges owing to the curvature discontinuity is discerned through the WA.

In order to successfully identify damage through spatial wavelet analysis, precise and spatially dense monitored data are necessary. In the last decades, a number of researchers have focused on developing replacements for traditional sensors (e.g. accelerometers, strain gages, load cells), which have the limitation of measuring the relevant parameters at a single location and of requiring cumbersome wiring. The modern measurement techniques, on the other hand, can capture the spatial field of the relevant parameters with high precision and in a quasi-continuous manner, even for large civil engineering structures. Such techniques include the Digital Imagine Correlation (DIC) and the digital imagine stereo-correlation (3D-DIC) [11-13], Global Positioning Systems

(GPS) [14-15], Local Positioning Systems (LPS) [16-17], scanning laser vibrometers [18-19] and optic fiber sensors [20-21].

In order to fully exploit the potential and versatility of the spatial wavelet analysis when quasi-continuous spatial measurement data are available, the present investigation is centered on the impact of the spatial sampling of beam deflection shapes in detecting damage. The state of the art highlights that in vibration-based damage detection methods the issue of selecting an appropriate sampling interval to discretize operational deflection shapes is well known, but few authors have investigated it in-depth.

Sazonov and Klinkhachorn [22] provide analytical and numerical arguments to select the optimal modeshape sampling interval to maximize sensitivity to damage and accuracy of damage localization. They highlight that the effects of measurement noise invalidate the intuitively reasonable idea that smaller sampling intervals mean higher precision in damage localization. Guan and Karbhari [23], noticing that modal curvature methods exhibit problems related to large sampling intervals and that measurement noise increase with numerical differentiation procedures, propose a new damage identification method based on the concept of element modal strain damage index which is able to correctly locate a damage region even using sparse measurements of noisy data. Zhong and Oyadiji [24] analyze the sampling interval sensitivity for damage detection in simply supported cracked beams using three different methods based on the Stationary Wavelet Transform (SWT). They search for the proper sampling distance as a function of depth, width and location of the crack as well as of the amount of noise. The proposed methods are shown to be robust if higher mode shapes are considered and to be accurate if the sampling interval with respect to the beam length is equal or less than 0.01. In Refs [25-26], Surace et al. deal with the problem of crack localization in post-damage operational beam shapes through a method based on a polynomial annihilation technique. Through numerical simulations, they quantify the number of sampling points (19 to 100 sampling points are considered) needed for damage detection. Whilst in absence

of noise, even with few measurement points (e.g. 25 data points), a small-medium crack can be located, with increased noise level cracks can be identified only by using smaller sampling intervals. Many authors [9, 27-28] observe that in the presence of course sampling intervals, damage detection may encounter difficulties when CWT is used. To overcome the problem, they adopt the technique of over-sampling the measured data through a cubic spline interpolation.

The present paper addresses the spatial CWT based damage identification in beam structures with the aim of answering the following key questions: (i) can the cost of damage detection be reduced by down-sampling? (ii) what is the minimum number of sampling intervals required for optimal damage detection? The first three free vibration modes of cantilever and simple supported beams with an open edge crack are considered (note that this study focuses on beams of constant cross-section, characterized by homogeneous isotropic material and linear elastic behaviour). An in-depth investigation of the effect of the spatial sampling of the beam modeshapes in identifying the damage through the spatial CWT is carried out with reference to the minimum detectable crack. The relevant aspects of the problem, such as the padding methods to reduce border distortions [29-31], the mother wavelet functions (i.e. Coiflet and Gaussian of order 4, Daubechies of order 2 and real Morlet [32]), the crack depth and its location along the beam, the level of noise (simulated by synthetic Gaussian white noise) and the mechanical and geometrical beam parameters, are identified and are made to vary. The results are discussed in detail and the optimal number of sampling intervals for an effective damage detection is assessed.

2. MODELLING OF THE CRACKED BEAM

A cracked Euler-Bernoulli beam characterized by an open edge crack under different boundary conditions at the two ends, i.e. clamped-free (cantilever beam) and supported-supported (simply supported beam), is considered (Fig. 1). The free vibration responses are analytically evaluated by solving the free vibration equations of the two uncracked sub-beams connected by a rotational

spring (representing the local stiffness k_c of the cracked cross-section of the beam) at the crack location x_c. The beam has a rectangular cross-section with height h and width b; the crack depth is a and L is the beam length. The symbols I, A, E and ρ represent, respectively, moment of inertia and area of the cross-section and Young's modulus and density of the material.

Fig. 1 - Sketch of the two cracked beams under study.

The free vibration equation related to the two uncracked parts of the beam can be written as

$$EI\frac{\partial^4 v(x,t)}{\partial x^4}+\rho A\frac{\partial^2 v(x,t)}{\partial t^2}=0\,, \tag{1}$$

where $v(x, t)$ is the transversal displacement of the beam from its static equilibrium position at a distance x from the left end at the time t. Separating the variables in Eq. (1) ($v(x,t)=\eta(x)\,g(t)$) and solving the characteristic equation function of x, the modeshapes η_L and η_R of the left and right sub-beam, respectively, are as follows

$$\eta_L = C_{1L}sen(\alpha x)+C_{2L}\cos(\alpha x)+C_{3L}senh(\alpha x)+C_{4L}\cosh(\alpha x) \qquad 0\le x\le x_c \tag{2.1}$$

and

$$\eta_R = C_{1R}sen(\alpha x)+C_{2R}\cos(\alpha x)+C_{3R}senh(\alpha x)+C_{4R}\cosh(\alpha x) \qquad x_c\le x\le L\,, \tag{2.2}$$

where $\alpha=\left(\frac{\rho A\omega^2}{EI}\right)^{1/4}$ and ω is the natural frequency of the cracked beam.

The $C_{(.)}$ terms are integration constants arising from the solution of the fourth order differential equation in space. By imposing the boundary conditions (see Eqs 3 below), a system of eight linear equations is formed. The natural frequencies of the cracked beam are found by setting the determinant of the matrix of the linear system to zero and solving it numerically for the roots of α. The coefficient C_{1L} is imposed to be equal to unity.

The boundary conditions of the cantilever beam at the clamped and at the free end are, respectively:

$$\eta_L(0) = 0 \quad \text{and} \quad \eta'_L(0) = 0\,, \tag{3.1}$$

$$\eta''_R(L) = 0 \quad \text{and} \quad \eta'''_R(L) = 0\,. \tag{3.2}$$

The boundary conditions of the simple supported beam at the two ends are:

$$\eta_L(0) = 0 \quad \text{and} \quad \eta''_L(0) = 0\,, \tag{3.3}$$

$$\eta_R(L) = 0 \quad \text{and} \quad \eta''_R(L) = 0\,. \tag{3.4}$$

For both the beams, the conditions of continuity of displacement, moment and shear at the crack location can be expressed as

$$\eta_L(x_c) = \eta_R(x_c)\,, \quad \eta''_L(x_c) = \eta''_R(x_c) \quad \text{and} \quad \eta'''_L(x_c) = \eta'''_R(x_c)\,. \tag{3.5}$$

The rotational spring at the cracked section introduces a discontinuity of the rotation which can be written as

$$\eta'_R(x_c) - \eta'_L(x_c) = \frac{EI}{k_c}\eta''_R(x_c)\,. \tag{3.6}$$

The local stiffness k_c is evaluated, according to linear elastic fracture mechanics concepts, through the following expression [33]

$$, k_c = \frac{bh^2 E}{24\left(\delta/(1-\delta)\right)^2 (5.93 - 19.69\delta + 37.14\delta^2 - 35.84\delta^3 + 13.12\delta^4)} \tag{4}$$

where $\delta = a/h$ is the relative crack depth.

3. DAMAGE DETECTION BY SPATIAL CWT

3.1. Wavelet Analysis

Due to its multi-resolution properties, wavelet analysis, acting as a signal microscope, appears to have a better ability to analyze the details of non-stationary signals in comparison to traditional analysis tools, such as Fourier Transform or Short-Time Fourier Transform.

A wavelet function $\psi(x)$ is a zero mean local wave-like function which decays rapidly and satisfies particular conditions [1]. A family of wavelet functions can be obtained by considering:

$$\psi_{k,s}(x) = \frac{1}{\sqrt{s}}\psi\left(\frac{x-k}{s}\right), \tag{5}$$

where s and k are, respectively, the scale and the translation parameter. The continuous wavelet transform of a signal $\eta(x)$ with respect to the wavelet function $\psi(x)$ is defined as

$$W(k,s) = \int_{-\infty}^{+\infty} \eta(x)\frac{1}{\sqrt{s}}\psi^*\left(\frac{x-k}{s}\right)dx \tag{6}$$

where ψ^* is the complex conjugate of ψ.

Since the identification of a discontinuity in a function or in any of its derivatives can be linked to the number of vanishing moments of the analyzing wavelet function (e.g. see Ref. [34]), it is possible for a wavelet transform to detect singularities by choosing an appropriate basis function $\psi(x)$. Since the presence of an open crack in a beam may introduce a singularity in the derivatives of the deflected shape, wavelet transform is deemed to be a powerful tool to locate the damage. Due to the presence of the singularity, a wavelet transformed deflected shape yields a local variation or extremum of the wavelet coefficient at the location of damage throughout the different scales.

In the present study different wavelet functions, i.e. the 4th order Coiflets wavelet ('Coif4'), with 8 vanishing moments, the 2nd order Daubechies wavelet ('Db2') with 2 vanishing moments, the 4th order Gaussian wavelet ('Gaus4') with 4 vanishing moments, and the real Morlet wavelet ('Morl') [32], are used in the CWT in order to enlarge the investigation of the impact of the sampling interval in damage detection. Furthermore, a MATLAB routine to perform the CWT for the aforementioned wavelets is implemented by the authors to improve the accuracy of the existing built-in one (the original routine approximates the signal through a constant piecewise function, while the implemented one considers a linear piecewise trend) [35].

3.2. Noisy data simulation

Realistic situations are simulated in the following by superimposing noise to the signal corresponding to the beam deflection obtained from the mechanical model described in Section 2. It should be borne in mind that, in the ideal situation of no noise, wavelet analysis would actually be unnecessary to detect the damage position, since by numerically calculating the second derivative of the original signal the damage location can promptly be identified [36].

The presence of noise is simulated by adding a synthetic Gaussian white noise to the original response. To quantify the noise level, the signal to noise ratio (SNR) is considered. The SNR, expressed in decibels, is defined as

$$SNR = 10\log_{10}\left(\frac{P_{signal}}{P_{noise}}\right). \tag{7}$$

The term P with the subscripts in Eq. (7) denotes power and is computed as

$$P_{(.)} = \frac{1}{N_z}\sum_{i=1}^{N_z}\left|z(x_i)\right|^2, \tag{8}$$

where N_z denotes the number of discrete points of a generic sampled function $z(x)$.

3.3. Padding methods to reduce CWT edge effects

As above-mentioned, the CWT is defined by the convolution of the input signal $\eta(x)$ with a wavelet function generated by scaling and translating its mother wavelet $\psi(x)$. For a finite-length signal, when the convolution operation is executed close to the signal ends, the wavelet window extends into a region with no available data, so that the transform values close to the borders of the signal are tainted by the nonexistence of data. Consequently, the values of the CWT coefficients very close to the signal extrema arise abnormally (border distortions) and the real signal features of that region are consequently corrupted by the transform. As a result, edge effects can provoke the masking of the damage and yield false indicators.

To handle edge effects three extrema extension methods are considered in the following:

(i) the traditional linear padding method [29], which applies a linear extension, interpolating the first two and last two values of the beam deflection shape (Fig. 2a);

(ii) the isomorphism padding methods proposed by Messina [30], which extend the signal either through a polar-like symmetry (called "Rotation") when its second derivative tends to zero or a mirror symmetry (called "Turnover") when its first derivative tends to zero (Fig. 2b);

(iii) the polynomial extension method suggested by Montanari et al. [31], which pads the original signal by means of two high degree polynomial functions obtained through a fitting procedure. The extension functions satisfy continuity conditions and extend the trend of the noisy signal and its derivatives in an average sense (Fig. 2c).

Fig. 2 - A generic noisy data signal, $\eta(x)$, is extended through: (a) linear padding method [29], (b) isomorphism padding methods proposed by Messina [30]; (c) polynomial extension method proposed by Montanari et al. [31].

4. PARAMETRIC STUDY

The effect of the sampling interval of the cracked beam modeshape in damage detection through the spatial CWT is numerically analysed varying the relevant parameters of the problem, that is: the normalized sampling interval $\Delta x/L$ ($\Delta x/L$ is considered equal to 0.025, 0.01, 0.005, 0.0025, 0.001, 0.0005 and 0.00025), the noise level (SNR value is assumed equal to 130 dB, 100 dB or 70 dB), the padding method (see Section 3.3), the wavelet function (i.e. 'Coif4', 'Db2', 'Gaus4' and 'Morl'), the deformed shape of the beam (i.e. the first three modeshapes of the cantilever and of the simply supported beam) and the relative crack position along the beam (x_c/L is considered equal to 0.1, 0.3, 0.5, 0.7 or 0.9).

In this Section, a cracked beam of length L = 1 m with a rectangular cross-section of height h = 0.05L and width b = 0.5h, constituted by an elastic linear isotropic material of Young modulus E = 200 GPa and density ρ = 7850 kg/m^3, is considered. In Section 5, the influence of the beam parameters on the effect of the sampling interval in detecting the damage is analyzed. Note that, for the present 1m-long beam, normalized sampling intervals of 0.001, 0.0005 and 0.00025 would yield unrealistic distances between measurement points, but they are considered in the following simulations in order to explore a broad range of sampling intervals.

4.1. Criterion for minimum detectable crack size

In order to investigate the effect of sampling interval in CWT based damage detection, the minimum detectable (threshold) crack size for a given spatial sampling interval is obtained according to the following criterion based on an iterative procedure.

While increasing gradually the relative crack depth δ from a value of 0.0001 to 0.95, the wavelet transform is executed at fixed values of the scale s ($s = 2,4,6,\ldots,200$) and the maximum absolute value of the transform is determined for each scale. If for a given relative crack depth δ this maximum is attained for all scales at the crack position for each of an arbitrary number of 20 different random Gaussian white noise distributions, this value of δ can be regarded to be detectable, otherwise a larger value of δ has to be assessed. To allow for the numerical approximation of the CWT, the crack depth is also regarded as detectable even if the CWT absolute maximum is attained in either of the two nearest points (i.e. the preceding or the following point) to the actual damage location. For very small sampling intervals ($\Delta x / L < 0.005$), the criterion is relaxed to any of the four nearest points to the damage location.

The results pertaining to the effect of sampling interval on the minimum detectable crack size are presented in the following Sections (see the bilogarithmic graphs in Figs 3-9) as a function of the pseudo-frequency, $f_a = f_c/(\Delta x \cdot s)$, where f_c is the center frequency of the mother wavelet (i.e. the

frequency maximizing the Fourier transform of the mother wavelet modulus [29]). The values of center frequency f_c for the considered mother wavelets are: 0.6957 for 'Coif4', 0.6667 for 'Db2', 0.318 for 'Gaus4' and 0.8125 for 'Morl'.

4.2. Sampling effect varying the padding method

The present study deals with the effect of sampling interval on CWT near-edge crack detection (x_c/L = 0.1 is considered) using different padding methods (linear, Messina's and polynomial padding methods are analysed). The first modeshape of the cantilever beam is investigated and the 'Coif4' wavelet is used in the CWT.

Figures 3, 5 and 6 represent, for different noise levels and padding methods, the minimum detectable relative crack depth δ as a function of the data relative sampling distance $\Delta x/L$ and of the pseudo-frequency f_a. Graphs (a) refer to 'low' noise (SNR = 130 dB), graphs (b) to 'intermediate' noise (SNR = 100 dB) and graphs (c) to 'high' noise (SNR = 70). Note that the curves in Figs 3, 5 and 6 are plotted by considering an upper limit of δ equal to 0.95.

By juxtaposing the results reported in Figs 3, 5 and 6, it can be observed that the padding method significantly influences the relation between minimum detectable crack size and pseudo-frequency. When the linear padding method is used, considering $f_a \geq 12$ m^{-1}, at low noise level (SNR = 130 dB) the damage identification is a function of the pseudo-frequency only and not of the sampling interval (Fig. 3a). At higher noise levels, at a given value of pseudo-frequency larger sampling intervals are observed to be more effective in damage detection (see Figs 3(b,c)). This occurrence is attributable to be due to the linear extension method whose performance in reducing edge effects can decrease substantially in the presence of high noise and very small sampling step.

Moreover, considering $f_a \geq 12$ m^{-1}, the curves in Fig. 3 present a positive curvature with a minimum value, regardless of the sampling distance, at about the same pseudo-frequency equal to around 330, 60 and 12 m^{-1} for SNR equal to 130, 100 and 70 dB, respectively (note that in Figs 3(b-

c) for very low values of $\Delta x/L$ the positive curvature is not evident). This behavioral trend is caused by two reasons: the noise influence and the edge effects due to the linear padding. Moving from the high to low values of f_a, since high values of f_a are very sensible to noise, smaller cracks can only be detected until a minimum detectable crack size for certain level of noise is reached (the part of the curves to the right of the minimum value is ruled by the *presence of noise*). When decreasing beyond a certain value f_a, the wavelet detects the edge discontinuity due to the padding method (the part of the curves to the left of the minimum value is ruled by the *edge effects*).

Finally, as expected, the minimum detectable crack size tends to decrease with decreasing noise level.

Fig. 3 – Impact of the sampling interval in damage detection by spatial CWT with 'Coif4'. The linear padding method is used. The first modeshape of the cantilever beam with crack at $x_c/L = 0.1$ is analysed. (a) SNR = 130 dB; (b) SNR = 100 dB; (c) SNR = 70 dB.

At this point it might be worth explaining the reasons why for $f_a < 12$ m^{-1} the curves of Fig. 3 deviate from the behavioral trend described above, showing a vertical asymptote corresponding to about $f_a = 2.4$ m^{-1}. These reasons are related to the treatment of the edge effect at $x = 0$ using the linear padding method and the crack location close to that beam end ($x_c/L = 0.1$), as discussed in the following.

When the linear padding method is applied to a signal end with curvature different from zero (at $x = 0$ in the case of the cantilever 1st modeshape), the second derivative of the padded signal presents a severe discontinuity at that position [31]. Consequently, as shown in Fig. 4, the CWT analysis of the padded beam shape exhibits, when δ is smaller than a certain value, the highest coefficients close to the clamped end of the beam. For instance, using $s = 8$, corresponding to $f_a = 17.4$ m^{-1}, the highest value of the wavelet coefficients is at $x/L \cong 0.02$ when $\delta \leq 0.05$, while using s

= 52, corresponding to f_a = 2.7 m^{-1}, it is at $x/L = 0.1$, regardless of the value of δ (the blue curves related to δ = 0 in Fig. 4b are overlapped by the green and red ones). This means that, around the pseudo-frequency range $f_a = [2-4]$ m^{-1}, the CWT analysis does not detect the presence of tiny cracks but the discontinuity due to the linear padded method at x = 0 (Fig. 4b) and the vertical asymptotic trend of Fig. 3 takes place. On the other hand, as shown in Fig. 4a, by analyzing the signal by means of high pseudo-frequencies (f_a = 17.4 m^{-1} is used), for small crack sizes the wavelet analysis is more sensitive to the discontinuity due to the padding method, while for large crack size, the wavelet analysis is more sensitive to the crack discontinuity and the damage identification is satisfied. Analogous reasoning can be made for f_a smaller than about 1.3 m^{-1}.

Fig. 4 – Zoom of the normalized absolute values of the CWT coefficients obtained by analyzing the normalized first modeshape of the cantilever beam with crack at x_c/L = 0.1 varying the relative crack depth δ. The signals are sampled at $\Delta x/L$ = 0.005, considering SNR = 100 dB. Two different scales are considered: (a) s = 8, corresponding to f_a = 17.4 m^{-1} in Fig. 3; (b) s = 52, corresponding to f_a = 2.7 m^{-1} in Fig. 3.

In contrast to the results obtained with the linear padding method, when applying Messina's padding method, regardless of the noise level, the CWT- f_a curves for different values of $\Delta x/L$ tend to overlap and the damage identification becomes, with good approximation, a function of the pseudo-frequency only (see Fig. 5). This implies that, since the scale can be made to vary as desired, large sampling intervals can be as effective as small ones. As for linear padding with decreasing noise level, smaller cracks can be detected.

As in Fig. 3, the curves of Fig. 5 present a positive curvature with a minimum value, but now, given the smaller influence of border discontinuities on the CWT introduced by Messina's padding method [31], the curves of Fig. 5 attain their minimum value at a lower pseudo-frequency than that

observed in Fig. 3. The values of pseudo-frequency offering optimal damage detection are equal to around 45, 16 and 5 m^{-1} for SNR values equal to 130, 100 and 70 dB, respectively.

Fig. 5 – Impact of the sampling interval in damage detection by spatial CWT with 'Coif4'. Messina's padding method is used. The first modeshape of the cantilever beam with crack at x_c/L = 0.1 is analysed. (a) SNR = 130 dB; (b) SNR = 100 dB; (c) SNR = 70 dB.

By using the polynomial padding method [31], the damage identification turns out to be, with good approximation, a function of the pseudo-frequency only (in the simulations of Fig. 6 the fitting parameters of the method are assumed to be $\beta_1 = \beta_2 = 1$, $H_1 = \overline{H}_1$ and $H_2 = \overline{H}_2$). However the curves of Fig. 6 exhibit a different trend than those obtained with the linear and Messina's padding methods. Rather than being characterized by a positive curvature, they decrease monotonically from high to low pseudo-frequencies until, at a specific frequency, a sudden jump occurs toward the upper limit of δ (say, equal to 0.95). This specific value of pseudo-frequency represents, with good approximation, the *lowest* and *optimal* value of pseudo-frequency for damage identification (the optimal value is that allowing the minimum crack size to be detected as the pseudo-frequency is made to vary). It needs to be underlined that this lowest/optimal value of f_a is the same for all levels of noise. As shown further in Section 4.3, this result appears to occur when the polynomial padding method is used together with wavelet functions characterized by many vanishing moments.

The jump in the curves of Fig. 6 at the lowest/optimal value of f_a occurs because, by analyzing the cracked beam shape with wavelet functions characterized by lower pseudo-frequencies, even large cracks cannot be localized due to the influence of the edge effects. In Section 4.5 it will be illustrated that lower pseudo-frequencies can detect cracks located further away from the beam end,

but in any case below a certain value of f_a, damage detection fails due to the edge effects even in the presence of large cracks.

Figure 6 shows that the curves for $\Delta x/L$ = 0.00025 exhibit jumps to the upper limit of δ at a higher value of pseudo-frequency than those for larger sampling intervals. This trend is due to the fact that, when the crack is near the signal extremum, the wavelet analysis is tainted by edge distortions, and, particularly for very low sampling intervals, the maximum CWT coefficient value falls not exactly at the crack location (or at its two four nearest points, as permitted by the detection criterion), but at sampling points other from that of the crack location. In Section 4.5, it will be shown that when the crack is located far away from the beam ends, regardless of the value of the sampling interval, the lower bound of pseudo-frequency is the same.

Hereafter, due to its effectiveness and versatility in handling general shapes of beam deflection [31], the polynomial padding method is used and, since the minimum detectable crack size is effectively only f_a dependent, the results are shown as a function of the noise level only, irrespectively of the sampling interval. Note that, in order to reduce the computational cost, $H_1 = \overline{H}_1$ and $H_2 = \overline{H}_2$ is always imposed, but this assumption does not affect the results of this investigation.

The $f_{a,opt}$ is used to indicate the optimal value of pseudo-frequency f_a that gives the minimum detectable crack size ($f_{a,opt}$ is equal to about 12 m^{-1} in Fig. 6). The value $f_{a,opt}$ of pseudo-frequency approximately coincides, as shown above, with the lowest pseudo-frequency for performing damage detection.

Fig. 6 – Impact of the sampling interval in damage detection by spatial CWT with ‘Coif4’. The polynomial padding method is used. The first modeshape of the cantilever beam with crack at x_c/L = 0.1 is analysed. (a) SNR = 130 dB; (b) SNR = 100 dB; (c) SNR = 70 dB.

4.3. Sampling effect varying the wavelet function

Figure 7 displays the results of the sampling step impact in the CWT damage detection executed using the 2nd order Daubechies ('Db2'), the 4th order Gaussian ('Gaus4') and the Morlet ('Morl') wavelet functions. The first mode shape of the cantilever beam with crack at $x_c/L = 0.1$ is analysed.

Figure 7a shows that CWT damage identification by 'Db2', conversely to that by the other wavelet functions, depends on both '$\Delta x/L$' and f_a. In addition, 'Db2' exhibits a poor damage identification performance due to its characteristic of having only two vanishing moments [34]. Similarly to 'Coif4', using 'Gaus4' and 'Morl', the damage detection is, with good approximation, just pseudo-frequency f_a dependent in the medium-high f_a range. In particular, using 'Morl' the lower limit of f_a (corresponding to large values of '$\Delta x/L$') appears to be the smallest among those of the wavelet functions considered. The behavioral trend of results shown in Fig. 7 seems to be similar for the different SNR values considered.

The comparison with the results for 'Coif4' (see Fig. 6) demonstrates that 'Coif4' exhibit the best performances in damage detection in comparison to the other wavelet functions, and hence it is adopted throughout in the following.

Fig. 7 – Impact of the sampling interval in damage detection by spatial CWT varying the wavelet function. The polynomial padding method is used and the first modeshape of the cantilever beam with crack at $x_c/L = 0.1$ is analysed. (a) 'Db2'; (b) 'Gaus4'; (c) 'Morl'.

4.4. Sampling effect varying the modeshape

The second and the third mode shapes of the cantilever beam and the first three mode shapes of the simply supported beam are now analysed. The crack is located at $x_c/L = 0.1$. Figure 8 illustrates the effect of the sampling interval in CWT damage detection using 'Coif4' and the polynomial

padding method ($\beta_1 = \beta_2 = 1$ is used in Figs 8(a,c), $\beta_1 = 0.25$ and $\beta_2 = 0.33$ in Fig. 8b, $\beta_1 = \beta_2 = 0.5$ in Fig. 8d and $\beta_1 = \beta_2 = 0.3$ in Fig. 8e). The jumps in the curves at low frequencies are dependent on the analysed modeshape but, neglecting this disturbance due to edge effects, damage identification appears to be a function of f_a only. In Figs 8(a-e) the optimal pseudo-frequency $f_{a,opt}$ is, respectively, equal to about 11 m^{-1}, 18 m^{-1}, 12 m^{-1}, 16 m^{-1} and 21 m^{-1}.

Fig. 8 – Impact of the sampling interval in damage detection by spatial CWT with 'Coif4'. The polynomial padding method is used and different beam modeshapes with the crack at x_c/L = 0.1 are analysed. (a,b) second and third modeshape of the cantilever beam, respectively; (c,d,e) first, second and third modeshape of the simply supported beam, respectively.

4.5. Sampling effect for various crack locations

The effect of the sampling interval in the CWT damage detection is further investigated by varying the crack location: x_c/L = 0.3, 0.5, 0.7 and 0.9 are considered. The first modeshape of the cracked cantilever beam is analysed. By juxtaposing the results of Fig. 9 with those reported in Figs 3 to 8, the influence of border distortions in dictating the optimal value $f_{a,opt}$ of pseudo-frequency of the curves is clearly manifested. The further the crack location is from either beam end, the lower is the optimal pseudo-frequency $f_{a,opt}$. This means that damage detection can be achieved with a reduced number of sampling points. Furthermore, Figs 9(a-c) show that, since the crack is far away from the beam ends, the $f_{a,opt}$ is the same for each curve. In contrast in Fig. 9d, since the crack is close to the beam end (i.e. x_c/L = 0.9), a similar trend to that of Fig. 6d is shown. In Figs 9(a-d) the optimal pseudo-frequency $f_{a,opt}$ is, respectively, equal to about 6 m^{-1}, 2.5 m^{-1}, 6 m^{-1} and 12 m^{-1}.

Fig. 9 – Impact of the sampling interval in damage detection by spatial CWT with 'Coif4'. The

polynomial padding method is used; The first modeshape of the cantilever beam with a crack at different locations is analysed. (a) x_c/L=0.3; (b) x_c/L=0.5; (c) x_c/L=0.7; (d) x_c/L=0.9.

4.6. Discussion of the results

Focusing on the results of Sections 4.2 – 4.5, pertaining to the use of the polynomial padding method and the 'Coif4' wavelet, the following conclusions can be drawn:

(i) there is an optimal value of pseudo-frequency, independent of the noise level, which maximizes the performance of the damage detection for a given beam deflection shape and crack position;

(ii) by adjusting the wavelet scale, damage detection performances can be similar for small and large sampling intervals.

Considering that CWT based damage detection depends on the pseudo-frequency only, it is numerically illustrated how the use of the proper scale range is essential in detecting damage when different sampling intervals are considered [31].

The first modeshape of the cantilever beam, defined at the beginning of Section 4, with a crack of δ = 0.2 at x_c/L = 0.1 is analysed. The noise level is assumed to be equal to 70 dB. The same modeshape is sampled at $\Delta x/L$ = 0.01 and $\Delta x/L$ = 0.0004.

Figs 10(a,b) report the contour plots of the CWT ('Coif4' and the polynomial padding method with $\beta_1 = \beta_2 = 1$ are used) when the signal is sampled at $\Delta x/L$ = 0.01, and the scale ranges $s = [4-24]$ (i.e. $s = 4,5,6\ldots, 24$) and $s = [4-6]$ are respectively used. The CWT coefficients, considering the broad scale range, completely mask the crack location (Fig. 10a), which on the contrary can be identified using the narrow scale range (Fig. 10b).

Figures 10(c-d) highlight that even if the signal is sampled at an extremely small sampling interval ($\Delta x/L$ = 0.0004), the CWT damage detection can be achieved only considering a proper

scale range. The damage localization at the scale range $s=[2-40]$ fails (Fig. 10c), while it succeeds for $s=[96-158]$ (Fig. 10d).

The results reported in Fig. 10 are in agreement with those of Fig. 6c, which deal with the same beam deflection. Indeed Fig. 6c highlights that the optimal pseudo-frequency is in the range $f_a=[11-18]$ m^{-1}, which for $\Delta x/L$ = 0.01 corresponds to the scale range $s=[4-6]$, and for $\Delta x/L$ = 0.0004 to $s=[96-158]$.

Fig. 10 – Contour plots of the spatial CWT using 'Coif4' and the polynomial padding method (SNR = 70 dB). The first modeshape of the cantilever beam with crack of δ = 0.2 at x_c/L = 0.1 is analysed. Sampling interval $\Delta x/L$ and scale range are varied: (a) $\Delta x/L$ = 0.01, $s=[4-24]$; (b) $\Delta x/L$ = 0.01, $s=[4-6]$; (c) $\Delta x/L$ = 0.0004, $s=[2-40]$; (d) $\Delta x/L$ = 0.0004, $s=[96-158]$.

5. GENERALIZATION OF THE RESULTS

The results reported in Figs 3 to 9 in terms of minimum detectable crack size are related to beams characterized by particular values of the parameters ρ, h, b, L and E. In this Section, the influence of these beam parameters on the optimal pseudo-frequency in CWT based damage detection with the polynomial padding method and a fit wavelet function (e.g 'Coif4'), is analysed and a further generalization of the parametric study is obtained.

According to Eq. 2, the functions describing the general modeshape depend on the boundary conditions and on the parameter α, and in turns the corresponding natural frequency is a function of the material density ρ and of α. Hence, the material density ρ affects the natural frequencies of the cracked beam but not its mode shapes and it is not considered in the following.

Then, by substituting the LEFM expression of the local rotational stiffness k_c due to the crack (Eq. 4) in the boundary condition representing the rotation discontinuity at the crack section (Eq. 3.6), we obtain:

$$\eta_2'(x_c) - \eta_1'(x_c) = 2h\,\tilde{\mathrm{f}}(\delta)\,\eta_2''(x_c)\,, \tag{9}$$

where $\tilde{\mathrm{f}}(\delta) = \left(\delta/(1-\delta)\right)^2 (5.93 - 19.69\delta + 37.14\delta^2 - 35.84\delta^3 + 13.12\delta^4)$ is a function of the relative crack depth δ only. For a given beam deflection shape (and, hence, for a given value of the curvature in x_c, $\eta_1''(x_c) = \eta_2''(x_c)$), Equation 9 demonstrates that the rotation discontinuity due to the crack is a function of h and δ, but not of the other beam parameters b and E. Therefore, the CWT based damage detection results are invariant for constant values of h, δ, and L.,

As for the beam parameter h, it can be demonstrated [35] that its variation influences the detectable crack depth but not the optimal pseudo-frequency value of CWT damage detection. In summary, the optimal pseudo-frequency $f_{a,opt}$ is independent of the beam parameters b, h, E and ρ and hence, using the polynomial padding method and a given wavelet function, it is a function of the deformed beam shape and the crack position x_c. Formally, this can be written as:

$$f_{a,opt} = \mathrm{f}\,(\text{beam deflection shape}, x_c, L)\,. \tag{10}$$

Through the dimensional analysis and Buckingham's theorem [37], Eq. 10 can be expressed in the following dimensionless form:

$$f_{a,opt}^{*} = f_{a,opt}\,L = \mathrm{f}\,(\text{beam deflection}, x_c / L)\,, \tag{11}$$

Equation 11 states that the optimal pseudo-frequency $f_{a,opt}$ multiplied by the beam length L is a function of the beam deflection shape and the relative crack position x_c/L only.

Figure 11 illustrates the $f_{a,opt}^{*}$ against x_c/L curves pertaining to the first three modeshapes of the cantilever and simply supported beams. It can be noted that, mainly due to the edge effects, $f_{a,opt}^{*}$ turns out to be higher near the beam ends, especially for the third modeshapes.

Fig. 11 – Variation of $f^*_{a,opt}$ for the CWT damage detection with relative crack location for the first three modeshapes of: (a) cantilever beams; (b) simply supported beams.

According to the curves of Fig. 11, for a given wavelet scale, it is possible to calculate the optimal number of sampling intervals needed to detect the smallest crack located at x_c/L using a given beam vibration modeshape. For example, consider the requirement to monitor the service state of a cantilever of L = 5 m through the spatial CWT using the polynomial padding method and 'Coif4' wavelet. By analyzing the cantiliver's first modeshape (or operational shapes similar to the first modeshape), the optimum sampling interval to detect the smallest crack located more than 0.1m from the blade ends is $\Delta x = \frac{f_c\, L}{f^*_{a,opt}\, s} = \frac{0.6957 \cdot 50}{24 \cdot 2} \cong 0.072$ m, for s = 2.

Finally, from the definition of $f^*_{a,opt}$, the optimal number of sampling intervals yielding the best CWT damage detection at the scale s for a given crack location x_c/L, is equal to:

$$\left.\frac{L}{\Delta x}\right|_{opt} = \frac{f^*_{a,opt}\, s}{f_c}\,. \tag{12}$$

As an example, in Fig. 12 the minimum of such an optimal number of sampling intervals is considered by taking s = 2 (the value of s = 1 is discarded in the present study) and it is plotted as a function of x_c/L.

Fig. 12 – The minimum optimal number of beam sampling intervals, $L/\Delta x$, to perform the optimum CWT damage detection at scale s = 2 is plotted against the normalized crack location for the first three modeshapes of: (a) cantilever beams; (b) simply supported beams.

5. CONCLUSIONS

The present investigation examined the effect of the spatial sampling interval in damage detection by CWT, with the aim of answering the following key questions: Can the cost of damage detection be reduced by down-sampling? What is the minimum number of sampling intervals required for optimal damage detection? An in-depth parametric study has been carried out by analyzing the first three mode shapes of a cantilever and a simply-supported beam varying the relevant parameters of the problem, that is: the sampling interval, the noise level, the padding method, the wavelet function, the crack depth and position along the beam, and the mechanical and geometrical beam parameters.

The effect of the sampling interval in CWT based damage detection is investigated in terms of the minimum detectable crack size (which is defined on the basis of an ad-hoc criterion) as a function of the key parameter, pseudo-frequency. The padding method is observed to significantly influence the minimum detectable crack size. Using the linear padding method, where at low noise levels the damage detection is independent of the sampling interval, at medium-high noise levels small sampling intervals appear to be less effective. On the other hand, extending the deformed beam shape through Messina's methods or the polynomial padding method, regardless of the noise level, the damage detection is independent of the sampling interval and is a function of the pseudo-frequency only. Among the different wavelet functions being analyzed, 'Coif4' seems to be the most effective.

Focusing on the findings obtained using the polynomial padding method and 'Coif4' wavelet, curves of minimum detectable crack size against pseudo-frequency for different relative sampling intervals coincide and decrease monotonically with decreasing pseudo-frequency down to a lower bound value of pseudo-frequency f_a below which no damage detection is possible. This lower bound of f_a can be regarded as the optimal pseudo-frequency $f_{a,opt}$ capable of detecting the smallest crack size by CWT. The parametric study shows that such an optimal pseudo-frequency depends on

the modeshape and on the crack location along the beam. In addition, it has been observed that, for a given modeshape and crack position, different beam structures, characterized by the same value of x_c/L, attain the same optimal value of the dimensionless pseudo-frequency $f_{a,opt}L$.

In conclusion, even though modern measurement techniques allow beam deflection shapes to be monitored with very dense sampling points, down-sampling the measurement points reduces damage detection costs without affecting performance, as long as the optimal value of the pseudo-frequency can be achieved. The minimum optimal number of sampling intervals, corresponding to the wavelet scale equal to 2, can be determined in relation to the beam deflection shape and damage location. Finally, by performing the CWT analysis in the range of the optimal pseudo-frequency, down-sampling dense measured data can be used as a tool to verify the robustness of the results.

REFERENCES

[1] S. Mallat, A Wavelet Tour on Signal Processing, Academic Press, NewYork, 2001.

[2] Y. J. Yana, L. Cheng, Z. Y. Wua, L. H. Yam, Development in vibration-based structural damage detection technique. Mechanical Systems and Signal Processing, 21 (2007) 2198–2211.

[3] K. M. Liew, Q. Wang, Application of wavelet theory for crack identification in structures. Journal of Engineering Mechanics 124 (1998) 152–157.

[4] Q. Wang, X. Deng, Damage detection with spatial wavelets. International Journal of Solids and Structures 36 (1999) 3443–3468.

[5] A. Gentile, A. Messina, On the continuous wavelet transforms applied to discrete vibrational data for detecting open cracks in damaged beams. International Journal of Solids and Structures 40 (2003) 295–315.

[6] A. Messina, Detecting damage in beams through digital differentiator filters and continuous wavelet transforms. Journal of Sound and Vibration 272 (2004) 385–412.

[7] V. Pakrashi, B. Basu, A. O' Connor, A statistical measure for wavelet based singularity detection. Journal of Vibration and Acoustics 131(4) (2009).

[8] S. Loutridis, E. Douka, A. Trochidis, Crack identification in double cracked beams using wavelet analysis. Journal of Sound and Vibration 277(4) (2004) 1025–1039.

[9] M. Rucka, K. Wilde, Application of continuous wavelet transform in vibration based damage detection method for beams and plates. Journal of Sound and Vibration 297 (2006) 536–550.

[10] Q. Wang, N. Wu, Detecting the delamination location of a beam with a wavelet transform: an experimental study. Smart Material and Structures. 20(1) (2011) 012002.

[11] P. K. Rastogi, Optical Measurement Techniques and Applications. Artech House Inc., Boston, 1997.

[12] J.-J. Orteu, 3-D computer vision in experimental mechanics. Optics and Lasers in Engineering 47(3) (2009) 282-291.

[13] M. Ozbek, D. J. Rixen, O. Erne, G. Sanow, Feasibility of monitoring large wind turbines using photogrammetry. Energy 35(12) (2010) 4802-4811.

[14] F. Casciati, C. Fuggini, Engineering vibration monitoring by GPS: long duration records. Earthquake Engineering and Engineering Vibration 8(3) (2009) 459-467.

[15] A. Nickitopoulou, K. Protopsalti, S. Stiros, Monitoring dynamic and quasi-static deformations of large flexible engineering structures with GPS: Accuracy, limitations and promises. Engineering Structures 28(10) (2006) 1471-1482.

[16] F. Casciati, L. J. Wu, Investigating the potential of LPS in structural health monitoring. Proceedings of the Sixth International Conference on Wireless Communications Networking and Mobile Computing (WiCOM), IEEE, September 2010.

[17] F. Casciati, L. J. Wu, Global VS local positioning systems. Proceedings of the Fifth International Conference on World Conference on Structural Control and Monitoring 2010, Tokyo, July 2010.

[18] A. B. Stanbridge, D. J. Ewins, Modal testing using a scanning laser Doppler vibrometer. Mechanical Systems and Signal Processing 13(2) (1999) 255-270.

[19] S. Yang, M. S. Allen. Output-only modal analysis using continuous-scan laser Doppler vibrometry and application to a 20kW wind turbine, in: T. Proulx (Ed.), Modal Analysis Topics, vol. 3, Springer, New York, 2011, pp.47-64.

[20] H.-N. Li, D.-S. Li, G.-B. Song. Recent applications of fiber optic sensors to health monitoring in civil engineering. Engineering structures 26(11) (2004) 1647-1657.

[21] A. P. Adewuyi, Z. Wu, N. K. Serker, Assessment of vibration-based damage identification methods using displacement and distributed strain measurements. Structural Health Monitoring 8(6) (2009) 443-461.

[22] E. Sazonov, K. Powsiri, Optimal spatial sampling interval for damage detection by curvature or strain energy mode shapes. Journal of sound and vibration 285(4) (2005) 783-801.

[23] H. Guan, V. M. Karbhari, Improved damage detection method based on element modal strain damage index using sparse measurement. Journal of Sound and Vibration 309(3) (2008) 465-494.

[24] S. Zhong, S. O. Oyadiji, Sampling interval sensitivity analysis for crack detection by stationary wavelet transform. Structural Control and Health Monitoring 20(1) (2013) 45-69.

[25] C. Surace, G. Yan, R. K. Archibald, R. Saxena, R. Feng, Structural Damage Detection using the Polynomial Annihilation Edge Detection Method, Australian Journal of Structural Engineering (AJSE) 15(1) (2014), in press.

[26] C. Surace, R. Archibald, R. Saxena, On the use of the polynomial annihilation edge detection for locating cracks in beam-like structures. Computers & Structures 114 (2013) 72-83.

[27] E. Douka, S. Loutridis, A. Trochidis, Crack identification in beams using wavelet analysis, International Journal of Solid and Structures 40 (2003) 3557-3569.

[28] S. Zhong, S. O. Oyadiji, Detection of cracks in simply-supported beams by continuous wavelet transform of reconstructed modal data. Computers & structures 89(1) (2011) 127-148.

[29] M. Misiti, Y. Misiti, G. Oppenheim, J. Poggi, Wavelet Toolbox, The MathWorks Inc., 2000.

[30] A. Messina, Refinements of damage detection methods based on wavelet analysis of dynamical shapes. International Journal of Solids and Structures 45 (2008) 4068–4097.

[31] L. Montanari, B. Basu, A. Spagnoli, B. M. Broderick, A padding method to reduce edge effects for enhanced damage identification using wavelet analysis. Mechanical Systems and Signal Processing (2014), submitted.

[32] I. Daubechies, Ten lectures on wavelets, vol. 61, Society for Industrial and Applied Mathematics, Philadelphia, 1992.

[33] H. Tada, P. C. Paris, G. R. Irwin, The Stress Analysis of Crack Handbook. Del Research Corporation, St. Louis, 1985.

[34] V. Pakrashi, B. Basu, A. O'Connor. Structural damage detection and calibration using a wavelet–kurtosis technique. Engineering Structures 29 (2007) 2097-2108.

[35] L. Montanari, Vibration-based damage identification in beam structures through wavelet analysis, PhD Thesis, Univerity of Parma, 2014.

[36] A. K. Pandey, M. Biswas, M. M. Samman. Damage detection from changes in curvature mode shapes. Journal of Sound and Vibration 145(2) (1991) 321-332.

[37] H. L. Langhaar, Dimensional Analysis and Theory of Models, Wiley, New York, 1951.

Revised version, 18 November 2014

ON THE EFFECT OF SPATIAL SAMPLING IN DAMAGE DETECTION OF CRACKED BEAMS BY CONTINUOUS WAVELET TRANSFORM

Lorenzo MONTANARI, Andrea SPAGNOLI, Biswajit BASU, and Brian BRODERICK

LIST OF FIGURES

Fig. 1 - Sketch of the two cracked beams under study.

Fig. 2 - A generic noisy data signal, $\eta(x)$, is extended through: (a) linear padding method [29], (b) isomorphism padding methods proposed by Messina [30]; (c) polynomial extension method proposed by Montanari et al. [31].

Fig. 3 – Impact of the sampling interval in damage detection by spatial CWT with 'Coif4'. The linear padding method is used. The first mode shape of the cantilever beam with crack at x_c/L = 0.1 is analysed. (a) SNR = 130 dB; (b) SNR = 100 dB; (c) SNR = 70 dB.

Fig. 4 – Zoom of the normalized absolute values of the CWT coefficients obtained by analyzing the normalized first mode shape of the cantilever beam with crack at x_c/L = 0.1 varying the relative crack depth δ. The signals are sampled at $\Delta x/L$ = 0.005, considering SNR = 100 dB. Two different scales are considered: (a) s = 8, corresponding to f_a = 17.4 m^{-1} in Fig. 3; (b) s = 52, corresponding to f_a = 2.7 m^{-1} in Fig. 3.

Fig. 5 – Impact of the sampling interval in damage detection by spatial CWT with 'Coif4'. Messina's padding method is used. The first mode shape of the cantilever beam with crack at x_c/L = 0.1 is analysed. (a) SNR = 130 dB; (b) SNR = 100 dB; (c) SNR = 70 dB.

Fig. 6 – Impact of the sampling interval in damage detection by spatial CWT with 'Coif4'. The polynomial padding method is used. The first mode shape of the cantilever beam with crack at x_c/L = 0.1 is analysed. (a) SNR = 130 dB; (b) SNR = 100 dB; (c) SNR = 70 dB.

Fig. 7 – Impact of the sampling interval in damage detection by spatial CWT varying the wavelet function. The polynomial padding method is used and the first mode shape of the cantilever beam with crack at x_c/L = 0.1 is analysed. (a) 'Db2'; (b) 'Gaus4'; (c) 'Morl'.

Fig. 8 – Impact of the sampling interval in damage detection by spatial CWT with 'Coif4'. The polynomial padding method is used and different beam mode shapes with the crack at x_c/L = 0.1 are analysed. (a,b) second and third mode shape of the cantilever beam, respectively; (c,d,e) first, second and third mode shape of the simply supported beam, respectively.

Fig. 9 – Impact of the sampling interval in damage detection by spatial CWT with 'Coif4'. The polynomial padding method is used; The first mode shape of the cantilever beam with a crack at different locations is analysed. (a) x_c/L=0.3; (b) x_c/L=0.5; (c) x_c/L=0.7; (d) x_c/L=0.9.

Fig. 10 – Contour plots of the spatial CWT using 'Coif4' and the polynomial padding method (SNR = 70 dB). The first mode shape of the cantilever beam with crack of δ = 0.2 at x_c/L = 0.1 is analysed. Sampling interval $\Delta x/L$ and scale range are varied: (a) $\Delta x/L$ = 0.01, $s = [4-24]$; (b) $\Delta x/L$ = 0.01, $s = [4-6]$; (c) $\Delta x/L$ = 0.0004, $s = [2-40]$; (d) $\Delta x/L$ = 0.0004, $s = [96-158]$.

Fig. 11 – Variation of $f^*_{a,opt}$ for the CWT damage detection with relative crack location for the first three mode shapes of: (a) cantilever beams; (b) simply supported beams.

Fig. 12 – The minimum optimal number of beam sampling intervals, $L/\Delta x$, to perform the optimum CWT damage detection at scale s = 2 is plotted against the normalized crack location for the first three mode shapes of: (a) cantilever beams; (b) simply supported beams.

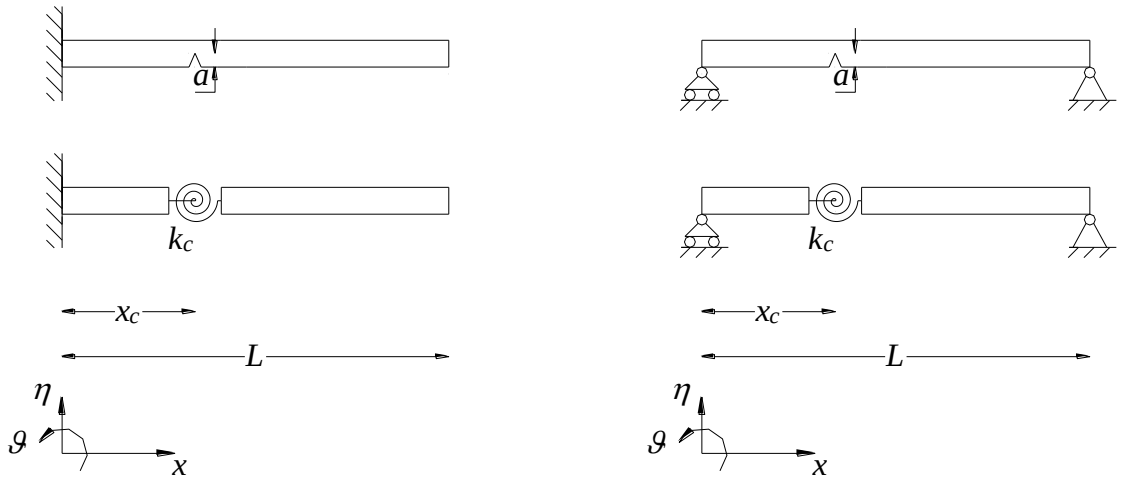

Fig. 1 - Sketch of the two cracked beams under study.

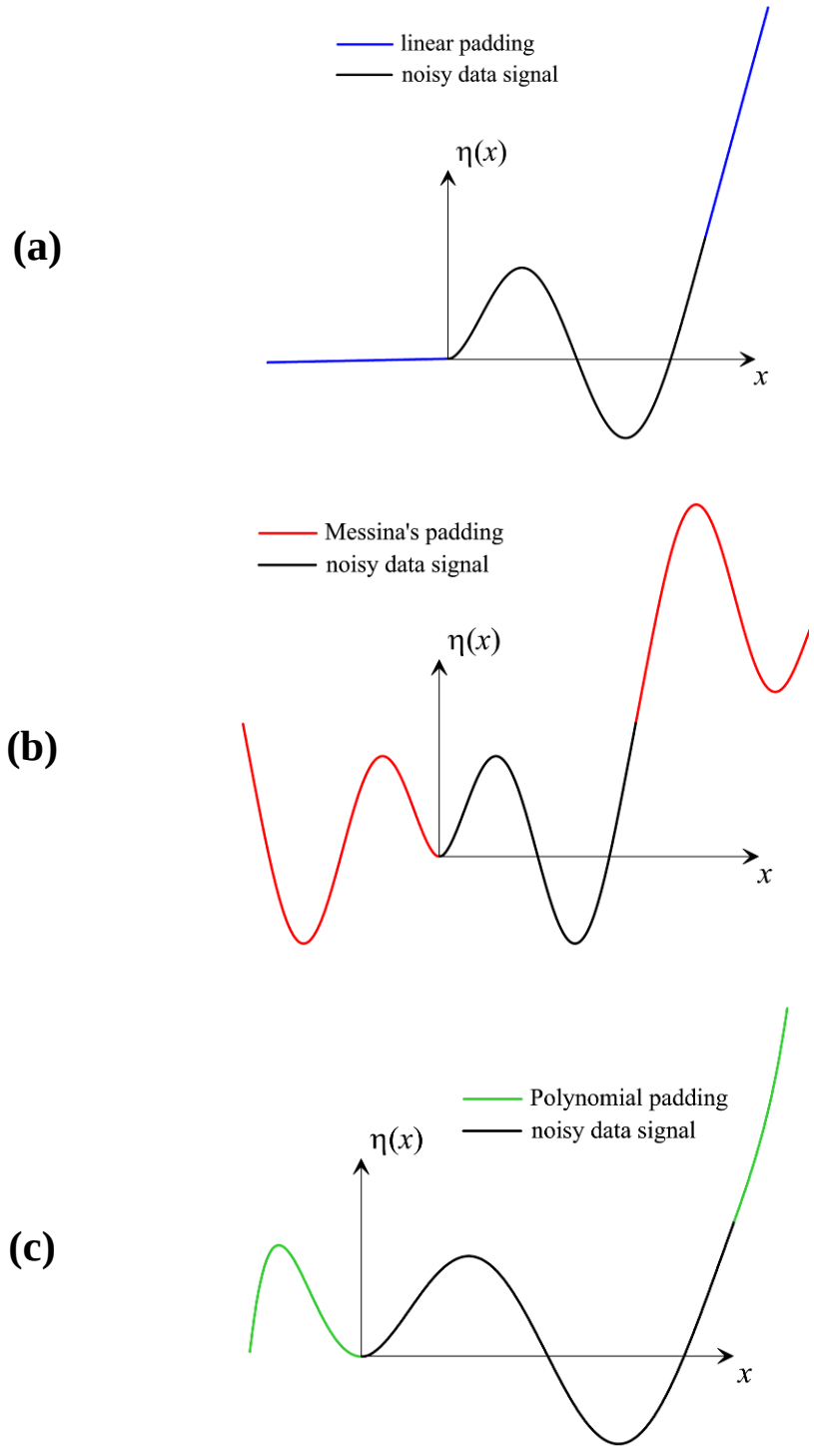

Fig. 2 - A generic noisy data signal, $\eta(x)$, is extended through: (a) linear padding method [29], (b) isomorphism padding methods proposed by Messina [30]; (c) polynomial extension method proposed by Montanari et al. [31].

(a)

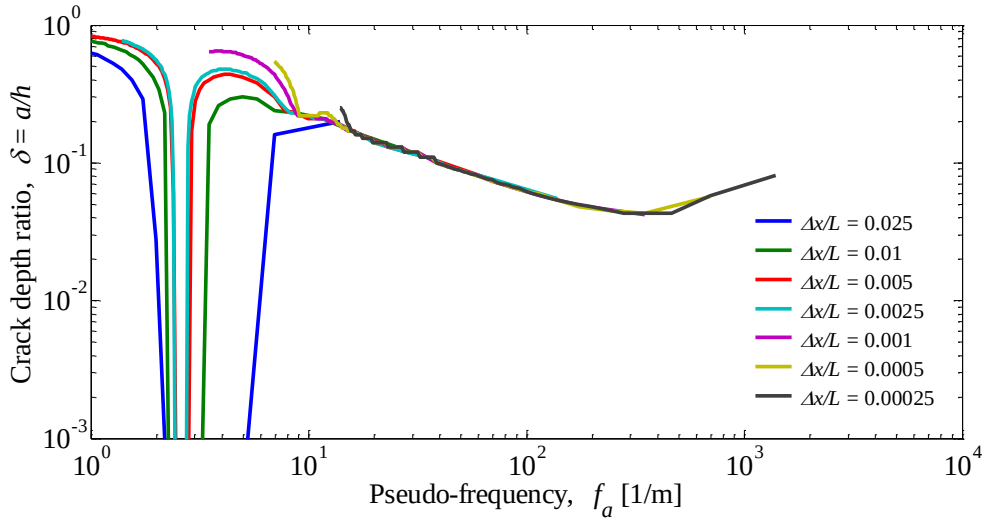

(b)

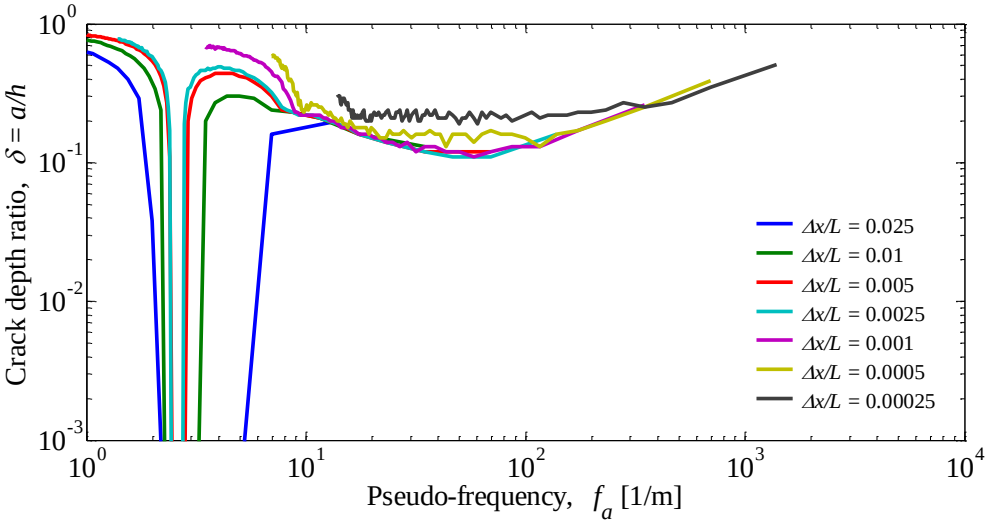

(c)

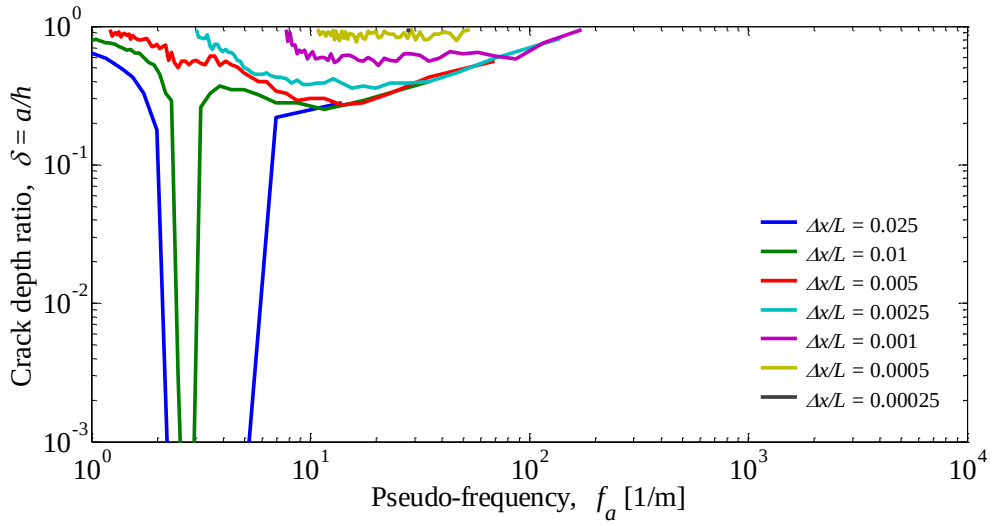

Fig. 3 – Impact of the sampling interval in damage detection by spatial CWT with 'Coif4'. The linear padding method is used. The first mode shape of the cantilever beam with crack at x_c/L = 0.1 is analysed. (a) SNR = 130 dB; (b) SNR = 100 dB; (c) SNR = 70 dB.

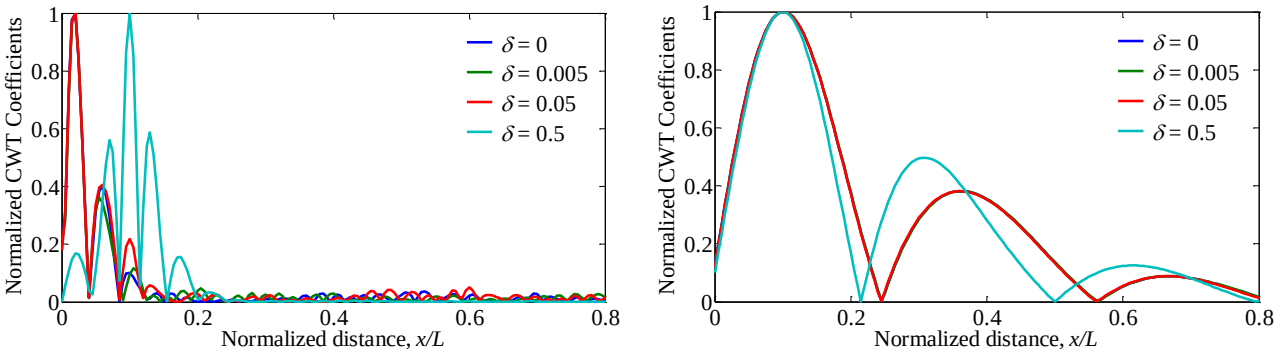

Fig. 4 – Zoom of the normalized absolute values of the CWT coefficients obtained by analyzing the normalized first mode shape of the cantilever beam with crack at x_c/L = 0.1 varying the relative crack depth δ. The signals are sampled at $\Delta x/L$ = 0.005, considering SNR = 100 dB. Two different scales are considered: (a) s = 8, corresponding to f_a = 17.4 m^{-1} in Fig. 3; (b) s = 52, corresponding to f_a = 2.7 m^{-1} in Fig. 3.

(a)

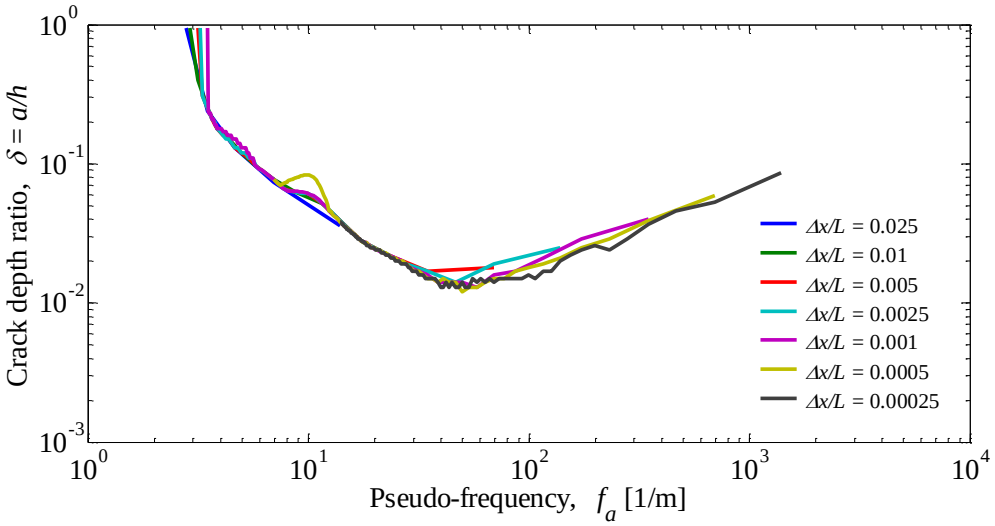

(b)

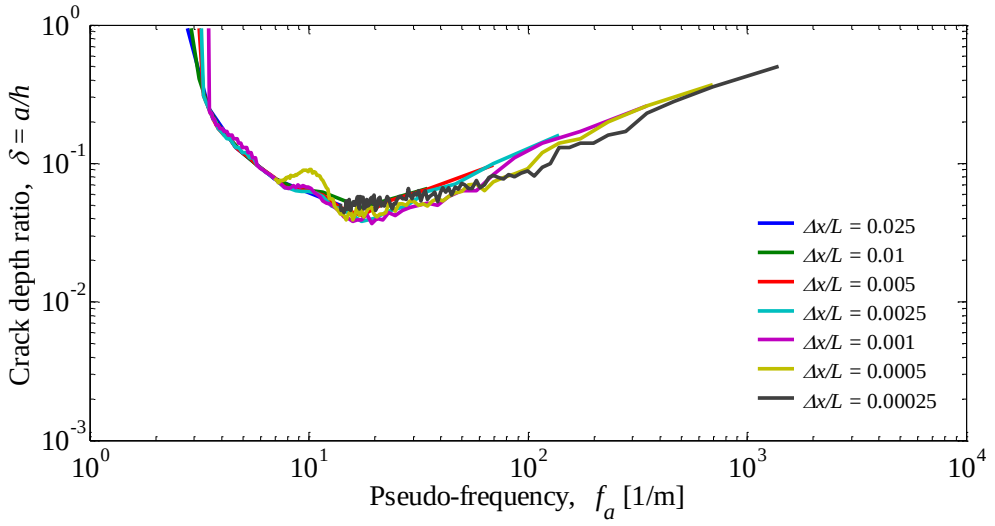

(c)

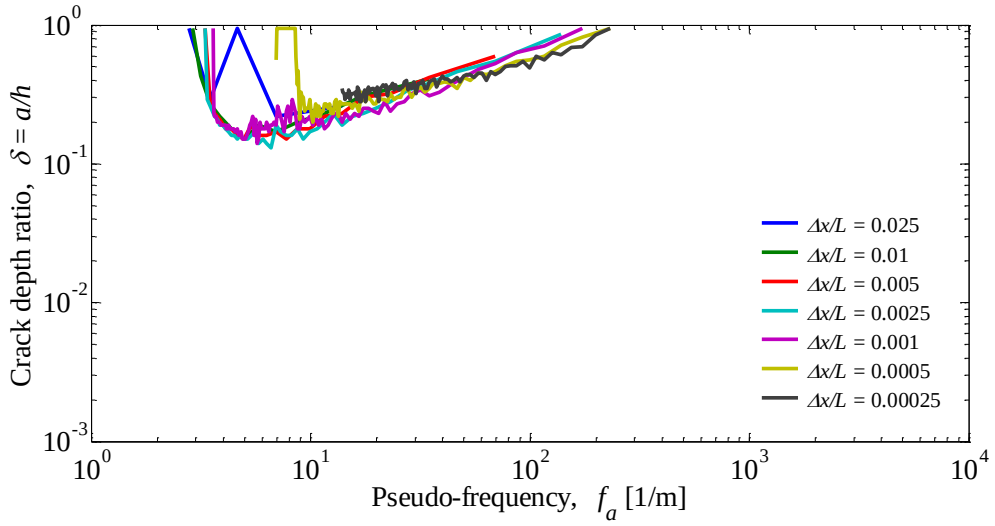

Fig. 5 – Impact of the sampling interval in damage detection by spatial CWT with 'Coif4'. Messina's padding method is used. The first mode shape of the cantilever beam with crack at x_c/L = 0.1 is analysed. (a) SNR = 130 dB; (b) SNR = 100 dB; (c) SNR = 70 dB.

(a)

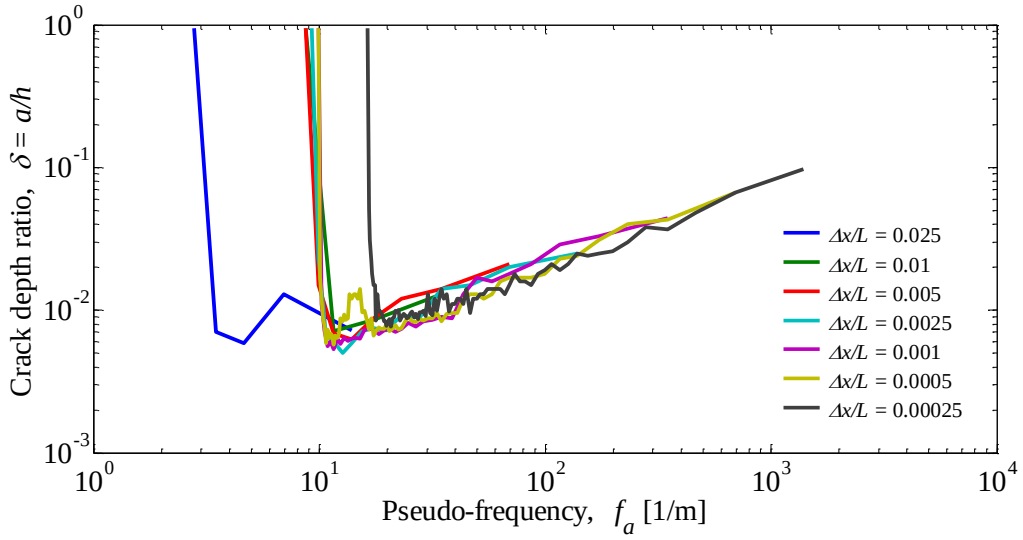

(b)

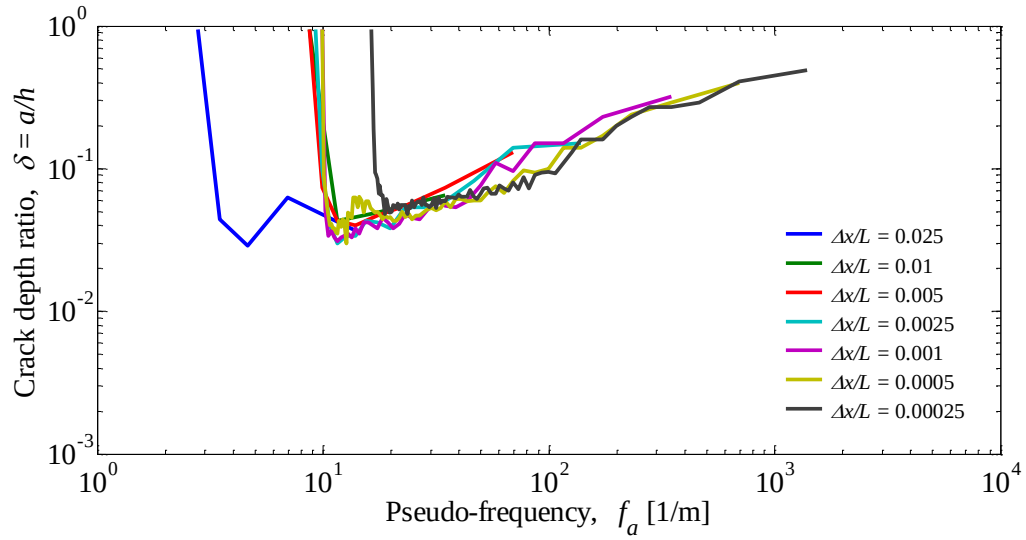

(c)

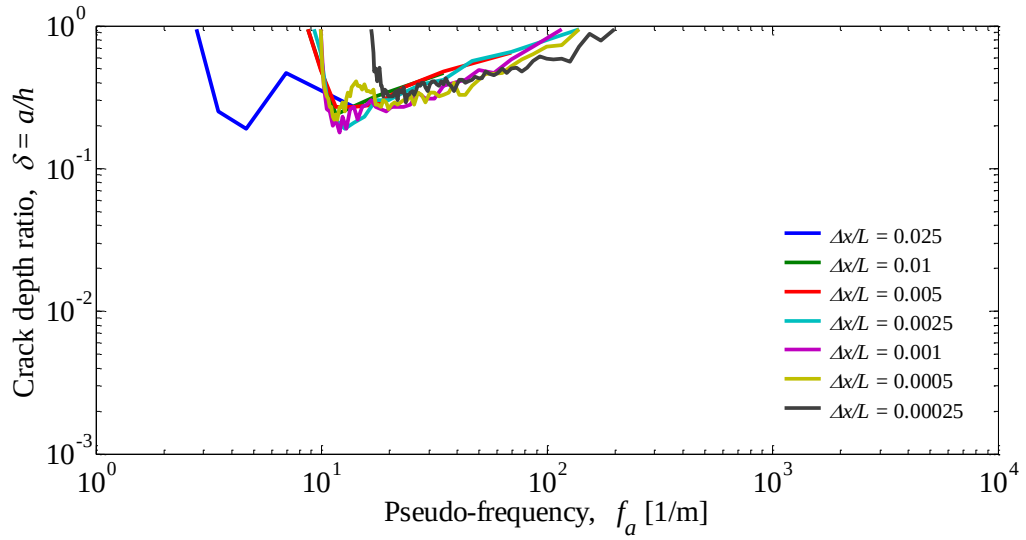

Fig. 6 – Impact of the sampling interval in damage detection by spatial CWT with 'Coif4'. The polynomial padding method is used. The first mode shape of the cantilever beam with crack at x_c/L = 0.1 is analysed. (a) SNR = 130 dB; (b) SNR = 100 dB; (c) SNR = 70 dB.

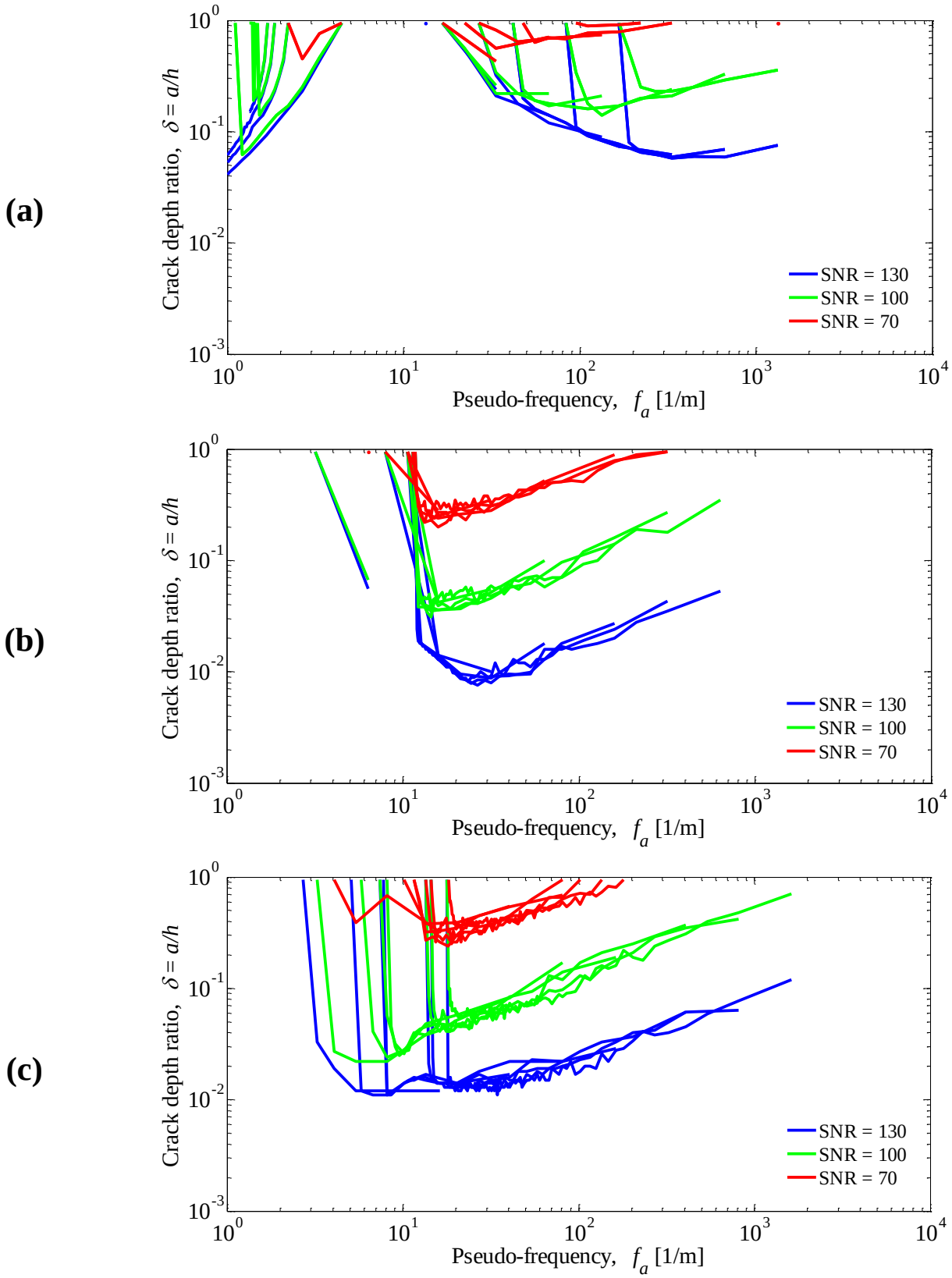

Fig. 7 – Impact of the sampling interval in damage detection by spatial CWT varying the wavelet function. The polynomial padding method is used and the first mode shape of the cantilever beam with crack at x_c/L = 0.1 is analysed. (a) 'Db2'; (b) 'Gaus4'; (c) 'Morl'.

(a)

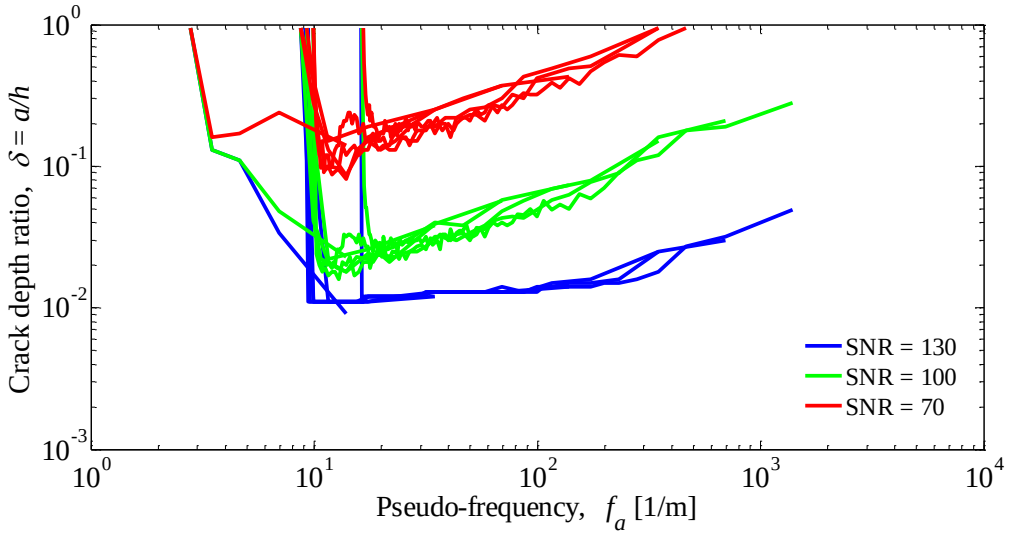
Crack depth ratio, $\delta = a/h$
Pseudo-frequency, f_a [1/m]
SNR = 130
SNR = 100
SNR = 70

(b)

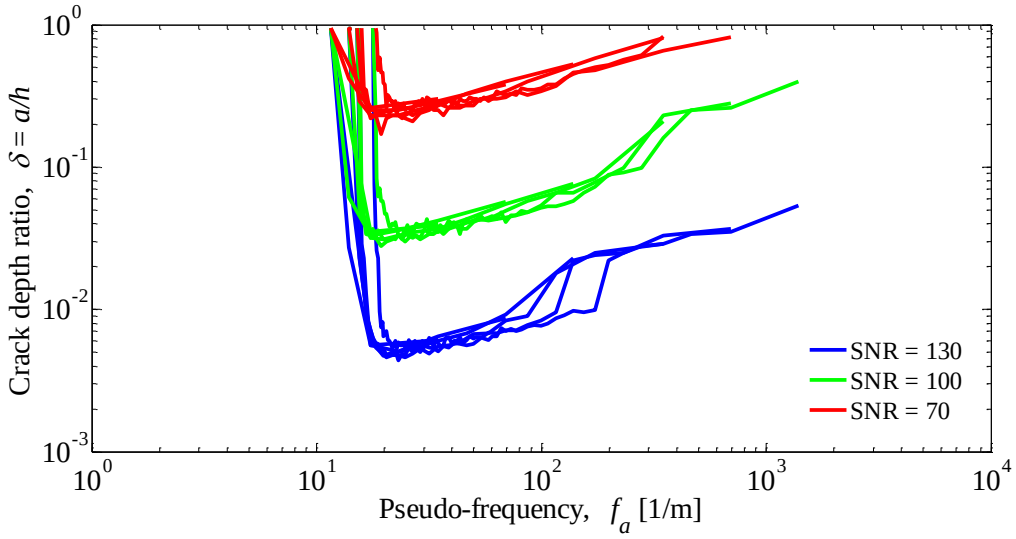
Crack depth ratio, $\delta = a/h$
Pseudo-frequency, f_a [1/m]
SNR = 130
SNR = 100
SNR = 70

(c)

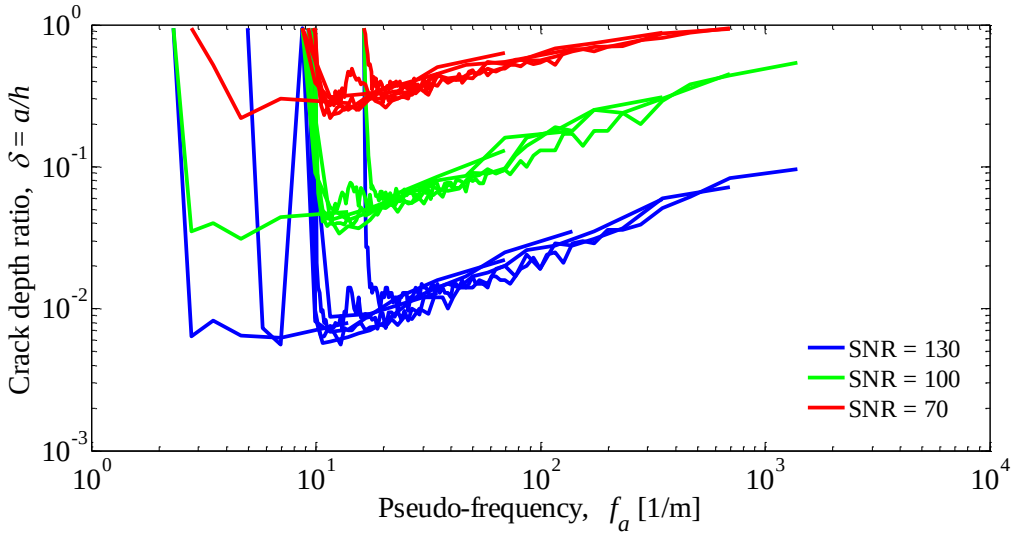
Crack depth ratio, $\delta = a/h$
Pseudo-frequency, f_a [1/m]
SNR = 130
SNR = 100
SNR = 70

Fig. 8(a-c)

(d)

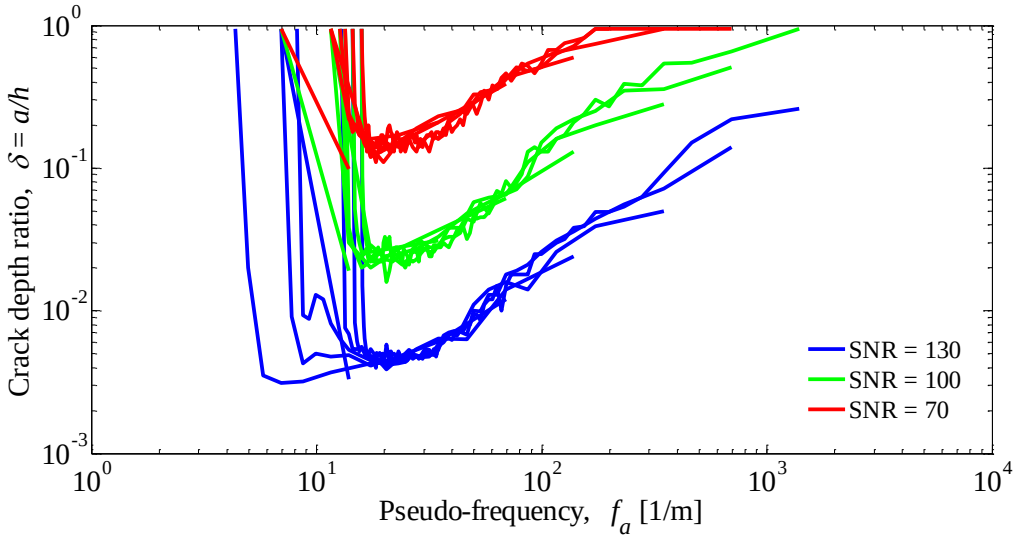

(e)

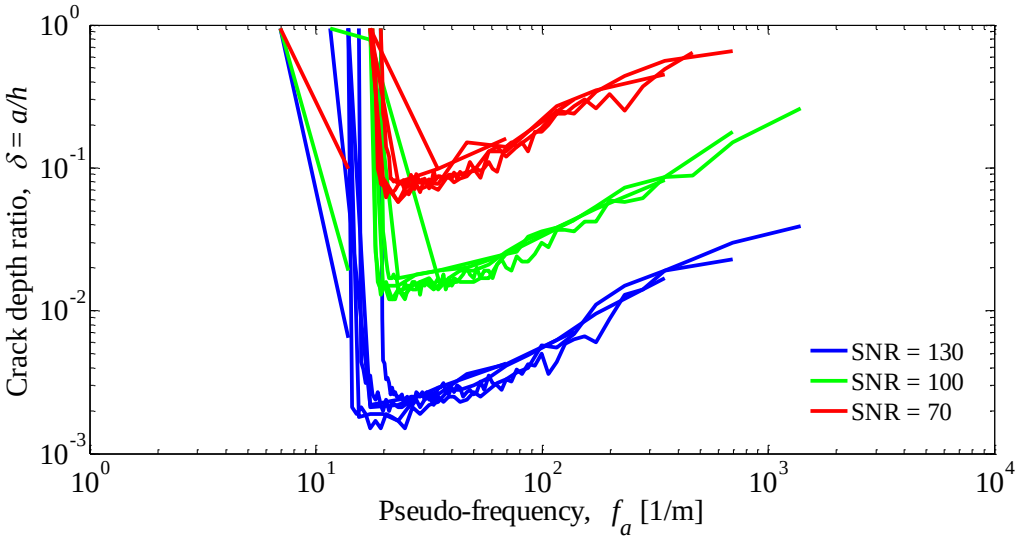

Fig. 8 – Impact of the sampling interval in damage detection by spatial CWT with 'Coif4'. The polynomial padding method is used and different beam mode shapes with the crack at $x_c/L = 0.1$ are analysed. (a,b) second and third mode shape of the cantilever beam, respectively; (c,d,e) first, second and third mode shape of the simply supported beam, respectively.

(a)

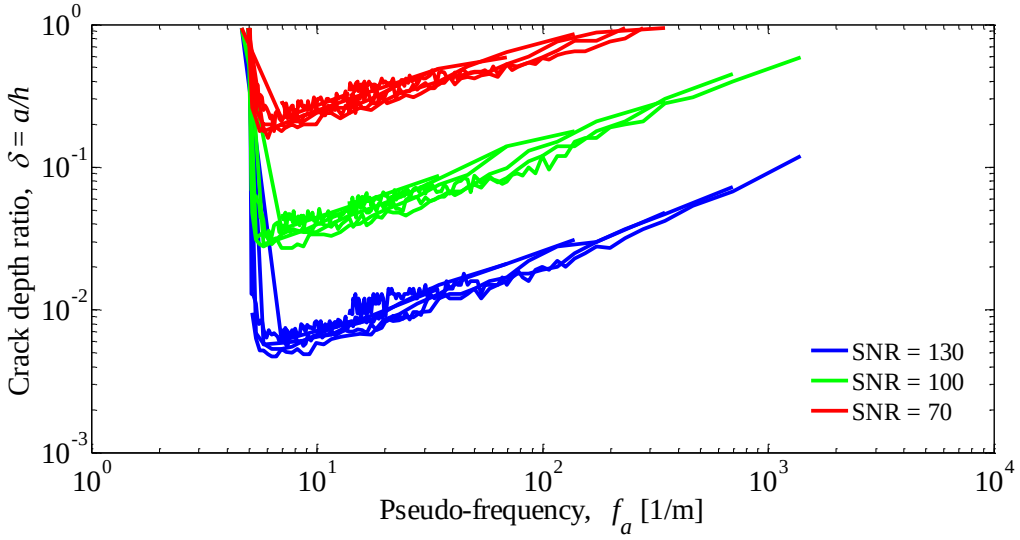
Crack depth ratio, $\delta = a/h$
Pseudo-frequency, f_a [1/m]
SNR = 130
SNR = 100
SNR = 70

(b)

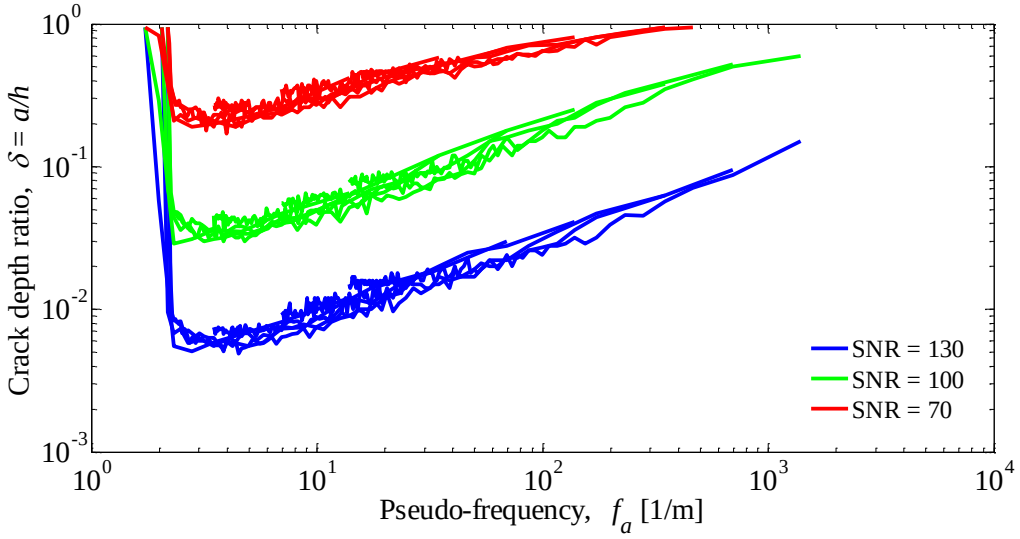
Crack depth ratio, $\delta = a/h$
Pseudo-frequency, f_a [1/m]
SNR = 130
SNR = 100
SNR = 70

(c)

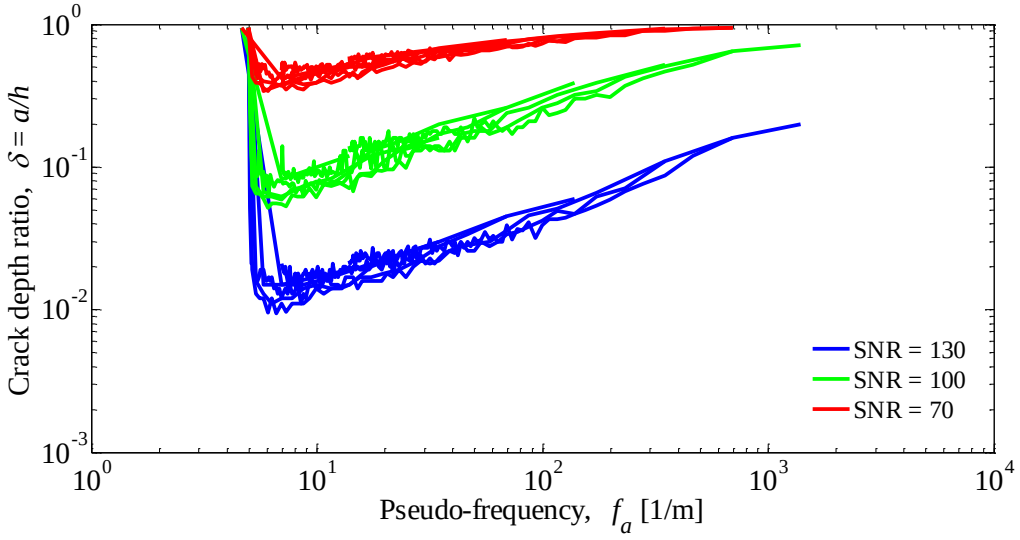
Crack depth ratio, $\delta = a/h$
Pseudo-frequency, f_a [1/m]
SNR = 130
SNR = 100
SNR = 70

Fig. 9(a-c)

(d)

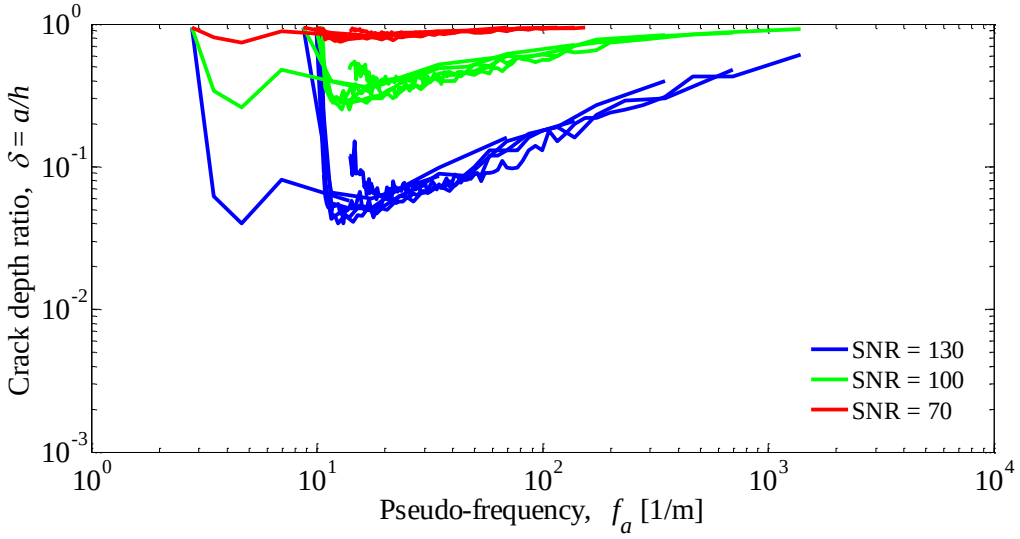

Fig. 9 – Impact of the sampling interval in damage detection by spatial CWT with 'Coif4'. The polynomial padding method is used; The first mode shape of the cantilever beam with a crack at different locations is analysed. (a) x_c/L=0.3; (b) x_c/L=0.5; (c) x_c/L=0.7; (d) x_c/L=0.9.

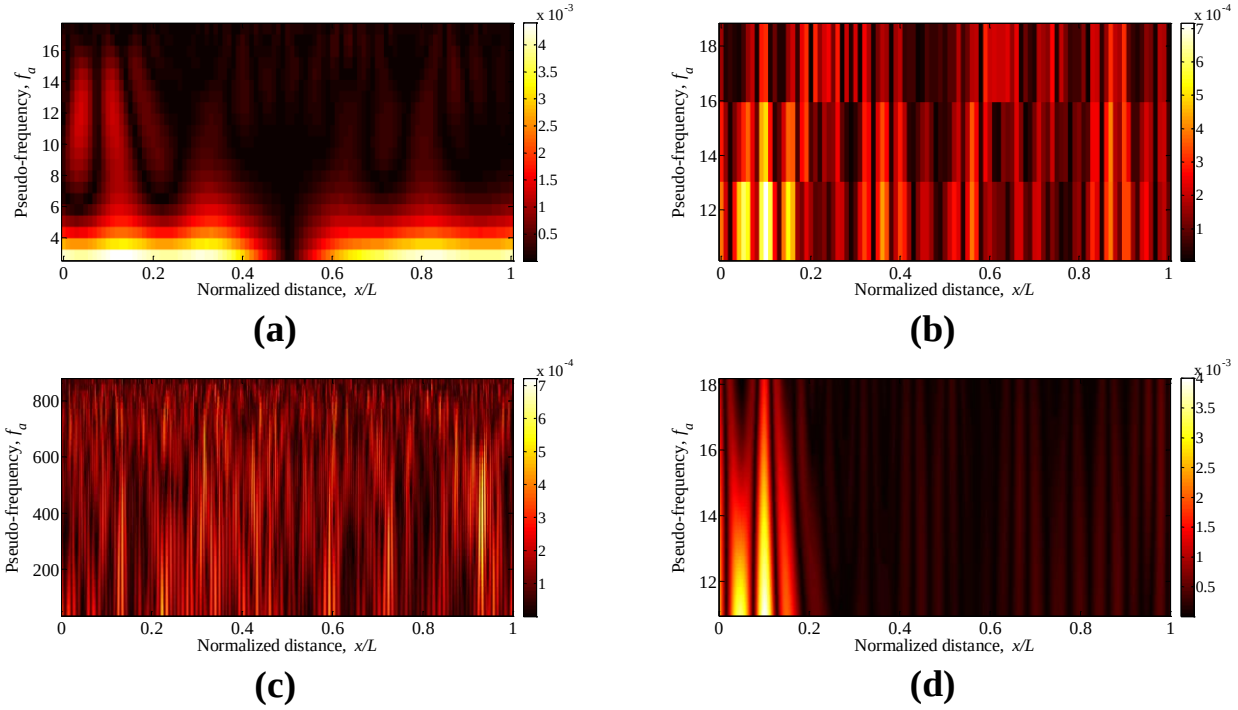

Fig. 10 – Contour plots of the spatial CWT using 'Coif4' and the polynomial padding method (SNR = 70 dB). The first mode shape of the cantilever beam with crack of δ = 0.2 at x_c/L = 0.1 is analysed. Sampling interval dx/L and scale range are varied: (a) $\Delta x/L$ = 0.01, $s = [4-24]$; (b) $\Delta x/L$ = 0.01, $s = [4-6]$; (c) $\Delta x/L$ = 0.0004, $s = [2-40]$; (d) $\Delta x/L$ = 0.0004, $s = [96-158]$.

(a)

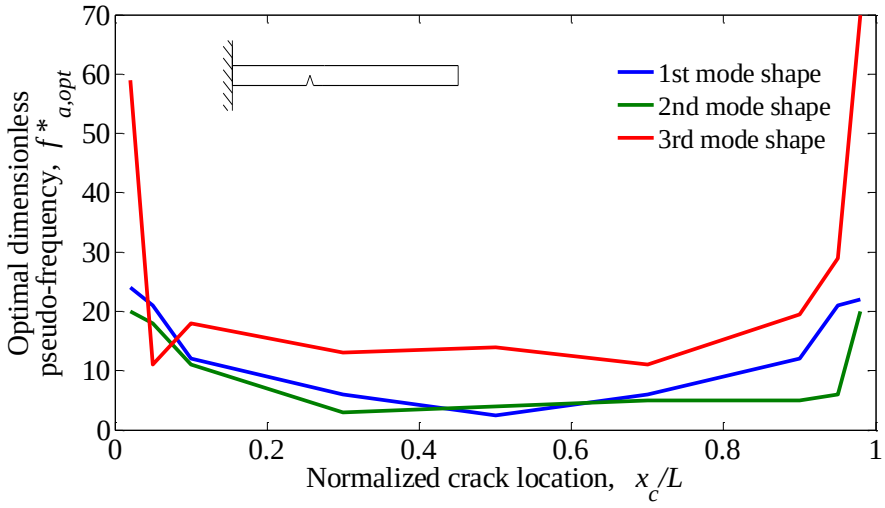

(b)

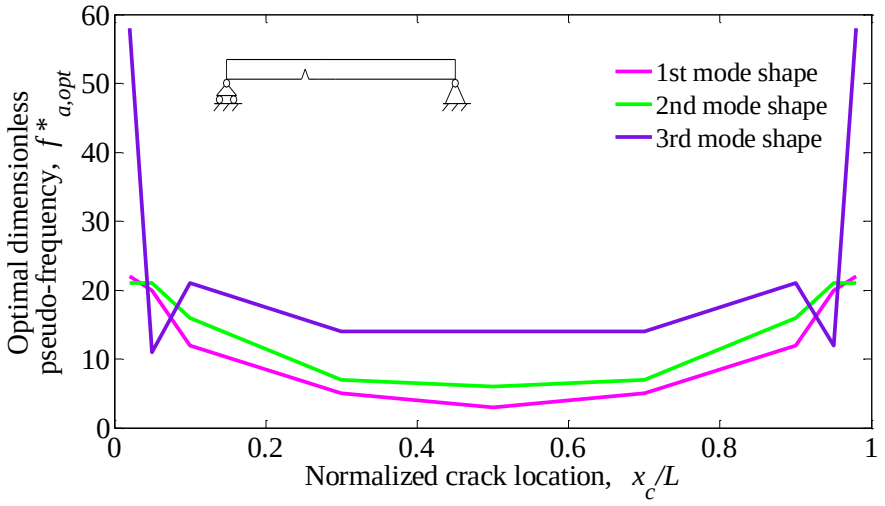

Fig. 11 – Variation of $f^*_{a,opt}$ for the CWT damage detection with relative crack location for the first three mode shapes of: (a) cantilever beams; (b) simply supported beams.

(a)

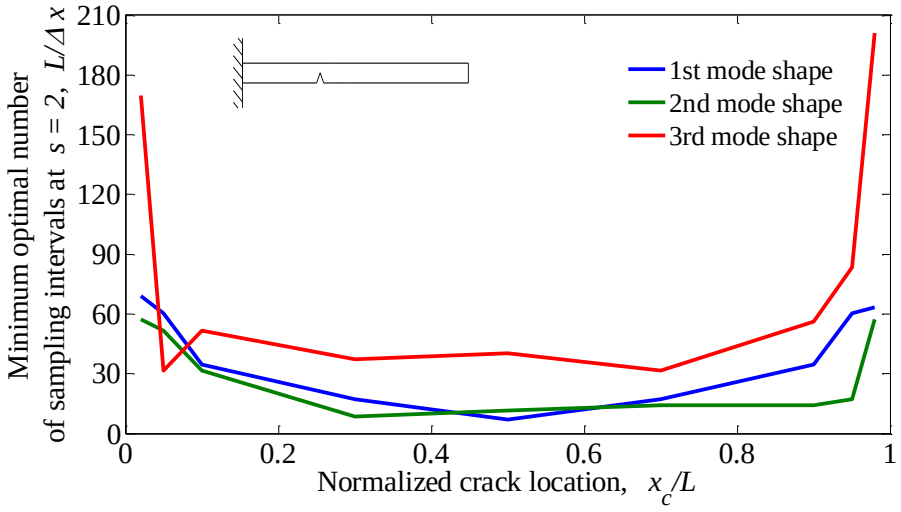

(b)

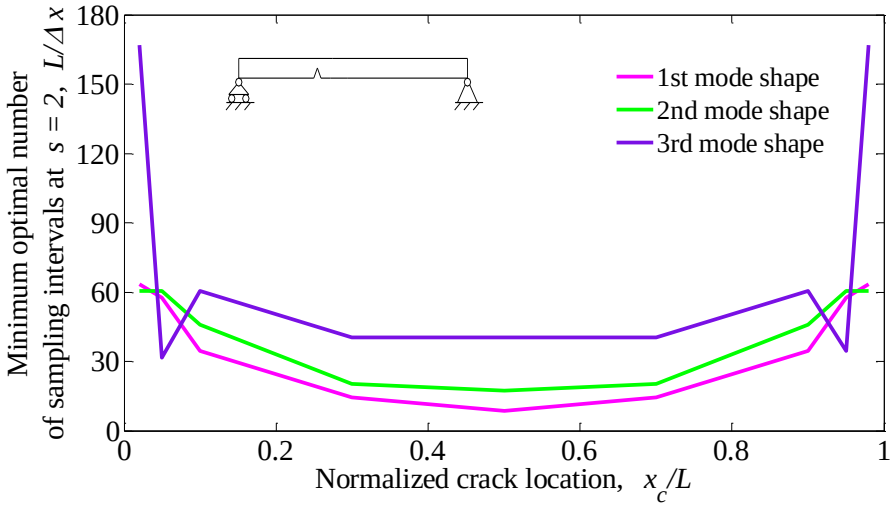

Fig. 12 – The minimum optimal number of beam sampling intervals, $L/\Delta x$, to perform the optimum CWT damage detection at scale $s = 2$ is plotted against the normalized crack location for the first three mode shapes of: (a) cantilever beams; (b) simply supported beams.